The topological derivative of stress-based cost functionals in anisotropic elasticity

Gabriel Delgado, Marc Bonnet

The topological derivative of stress-based cost functionals in anisotropic elasticity

Gabriel Delgado [a,b*], Marc Bonnet [c]

[a] CMAP, Ecole Polytechnique, Palaiseau, France
[b] Airbus Group Innovations, Suresnes, France
[c] POems (UMR 7231 CNRS-ENSTA-INRIA), ENSTA, Paris, France (*mbonnet@ensta.fr*)

Abstract

The topological derivative of cost functionals J that depend on the stress (through the displacement gradient, assuming a linearly elastic material behavior) is considered in a quite general 3D setting where both the background and the inhomogeneity may have arbitrary anisotropic elastic properties. The topological derivative $\mathrm{D}J(\boldsymbol{z})$ of J quantifies the asymptotic behavior of J induced by the nucleation in the background elastic medium of a small anisotropic inhomogeneity of characteristic radius a at a specified location $\boldsymbol{z}$. The fact that the strain perturbation inside an elastic inhomogeneity remains finite for arbitrarily small a makes the small-inhomogeneity asymptotics of stress-based cost functionals quite different than that of the more usual displacement-based functionals.

The asymptotic perturbation of J is shown to be of order $O(a^3)$ for a wide class of stress-based cost functionals having smooth densities. The topological derivative of J, i.e. the coefficient of the $O(a^3)$ perturbation, is established, and computational procedures then discussed. The resulting small-inhomogeneity expansion of J is mathematically justified (i.e. its remainder is proved to be of order $o(a^3)$). Several 2D and 3D numerical examples are presented, in particular demonstrating the proposed formulation of $\mathrm{D}J$ on cases involving anisotropic elasticity and non-quadratic cost functionals.

1 Introduction

The topological derivative $\mathrm{D}J(\boldsymbol{z})$ quantifies the perturbation induced to a cost functional J by the virtual creation of an object (in this work, an elastic inhomogeneity) occupying a region $B_a(\boldsymbol{z})$ with prescribed center $\boldsymbol{z}$ inside the solid and vanishingly small characteristic radius a. In structural optimization, the field $\mathrm{D}J(\boldsymbol{z})$ helps directing the algorithm towards optimal topologies by indicating where creating new holes is most profitable, see e.g. [6, 39] and also [1] in conjunction with the shape derivative. Moreover, computational evidence [11, 19, 33] as well as more recent theoretical and experimental studies [3, 12, 45] show that the topological derivative is also effective for flaw identification problems.

Most of the studies so far devoted to the topological derivative and its applications consider cost functionals that depend on the primary variable, namely the displacement field in the

*Current address: IRT System X, Palaiseau, France, *gabriel.delgado@irt-systemx.fr*

solid mechanics context of this work. Such formulations exploit the analysis of the asymptotic behavior as $a \to 0$ of the perturbation induced to the displacement by the virtual creation of $B_a(\boldsymbol{z})$, for which an abundant literature is available [4, 15, 16, 27, 34]. An important component of small-inhomogeneity asymptotics of displacement fields is the elastic moment tensor (EMT), whose definition and properties are studied in e.g. [5] for isotropic materials and [13, 38] for anisotropic materials.

However, some optimization problems involve stress-based cost functionals, which is equivalent (for the present context of linearly elastic solids) to considering functionals that depend on strains or displacement gradients. Examples include topology optimization of composite structures with materials constrained by yield criteria, and flaw identification using full-field kinematical measurements, as both types of problems may be cast as minimization problems involving stress-based cost functionals. The asymptotic behavior of such cost functionals is quite different, and more involved, than in the previous case, due to the fact that the strain perturbation inside an elastic inhomogeneity has a finite, nonzero limit as $a \to 0$, while the asymptotics of displacement-based functionals rests upon the fact that the magnitude of the displacement perturbation vanishes as $a \to 0$.

So far, only few works have investigated the small-inhomogeneity asymptotics of stress-based functionals. The 2D isotropic case is addressed for specific stress-based functionals (elastic energy, von Mises and Drucker-Prager yield criteria) in [7, 8, 41]. Moreover, results for general quadratic stress-dependent functionals are given in [40] within a 2D and 3D anisotropic framework. The special case of cost functionals that are directly linked to the anisotropic elastic potential energy in 2D or 3D is considered in [15]. The main purpose of this article is to formulate and justify the topological derivative for stress-dependent functionals, in a quite general three-dimensional framework where the functionals are defined in terms of domain integrals of arbitrary sufficiently smooth densities while both the background material and the small trial inhomogeneity are allowed to have anisotropic elastic properties. The results given herein for topological derivatives thus contain expressions given in [7, 8, 15, 41] as special cases. They are illustrated by computational experiments on 2D and 3D examples involving anisotropic elasticity and stress-based quadratic or non-quadratic cost functionals, and inspired by topology optimization or flaw identification.

The article is organised as follows. Section 2 recalls the concept of topological derivative, introduces notation and collects the main facts on the elastic transmission problem and elastic moment tensor. The main result on topological derivative is stated and established in Section 3. The numerical evaluation of $\mathrm{D}J$ is addressed in Section 4, and Section 5 is then devoted to the presentation and discussion of computational experiments.

2 Elastic transmission problem and cost functional

2.1 Notation, elastic transmission problem

Consider an elastic body occupying a smooth bounded domain $\Omega \subset \mathbb{R}^3$. The anisotropic elastic properties of the background material (against which the effect of small inhomogeneities will be considered), assumed to be homogeneous, are characterized by the fourth-order elasticity tensor $\boldsymbol{\mathcal{C}}$. The boundary $\partial\Omega$ is split according to $\partial\Omega = \Gamma_{\mathrm{D}} \cup \Gamma_{\mathrm{N}}$ (where $\Gamma_{\mathrm{D}} \cap \Gamma_{\mathrm{N}} = \emptyset$ and $|\Gamma_{\mathrm{D}}| \neq 0$), so that a given force density $\boldsymbol{g} \in L^2(\Gamma_{\mathrm{N}}; \mathbb{R}^3)$ is applied on Γ_{N} while a given displacement $\bar{\boldsymbol{u}} \in H^{1/2}(\Gamma_{\mathrm{D}}; \mathbb{R}^3)$ is prescribed on Γ_{D}. Additionally, a body force density $\boldsymbol{f}$

assumed (for reasons given later) to have $C^{0,\beta}(\Omega)$ Hölder continuity for some $\beta > 0$ is applied to Ω.

The background solution, i.e. the displacement field arising in the reference solid due to the prescribed excitations $(\boldsymbol{f}, \boldsymbol{g}, \bar{\boldsymbol{u}})$, is defined as the solution to

$$\operatorname{div}(\boldsymbol{\mathcal{C}} : \boldsymbol{\varepsilon}[\boldsymbol{u}]) + \boldsymbol{f} = \boldsymbol{0} \text{ in } \Omega, \quad (\boldsymbol{\mathcal{C}} : \boldsymbol{\varepsilon}[\boldsymbol{u}]) \cdot \boldsymbol{n} = \boldsymbol{g} \text{ on } \Gamma_{\mathrm{N}}, \quad \boldsymbol{u} = \bar{\boldsymbol{u}} \text{ on } \Gamma_{\mathrm{D}} \tag{1}$$

where $\boldsymbol{n}$ is the unit outward normal to Ω and $\boldsymbol{\varepsilon}[\boldsymbol{w}]$ denotes the linearized strain tensor associated with a given displacement $\boldsymbol{w}$, defined by

$$\boldsymbol{\varepsilon}[\boldsymbol{w}] = \tfrac{1}{2}(\boldsymbol{\nabla} \boldsymbol{w} + \boldsymbol{\nabla} \boldsymbol{w}^{\mathrm{T}}). \tag{2}$$

In (1) and hereinafter, symbols '$\cdot$' and ' : ' denote single and double inner products, e.g. $(\boldsymbol{\mathcal{C}} : \boldsymbol{\varepsilon})_{ij} = \mathcal{C}_{ijk\ell} \varepsilon_{k\ell}$, with Einstein's convention of summation over repeated indices implicitly used throughout.

Alternatively, the background displacement is governed by the weak formulation

$$\text{Find } \boldsymbol{u} \in W(\bar{\boldsymbol{u}}), \qquad \langle \boldsymbol{u}, \boldsymbol{w} \rangle_{\Omega}^{\mathcal{C}} = F(\boldsymbol{w}), \quad \forall \boldsymbol{w} \in W_0, \tag{3}$$

where $\langle \boldsymbol{u}, \boldsymbol{w} \rangle_{D}^{\mathcal{C}}$ denotes the bilinear elastic energy form associated to given domain $D \subset \mathbb{R}^3$ and elasticity tensor $\boldsymbol{\mathcal{C}}$, i.e.:

$$\langle \boldsymbol{u}, \boldsymbol{w} \rangle_{D}^{\mathcal{C}} := \int_D \boldsymbol{\varepsilon}[\boldsymbol{u}] : \boldsymbol{\mathcal{C}} : \boldsymbol{\varepsilon}[\boldsymbol{w}] \, \mathrm{d}V = \int_D \boldsymbol{\nabla} \boldsymbol{u} : \boldsymbol{\mathcal{C}} : \boldsymbol{\nabla} \boldsymbol{w} \, \mathrm{d}V \tag{4}$$

(with the second equality holding by virtue of the well-known minor symmetries of $\boldsymbol{\mathcal{C}}$), the linear form F associated to the loading is defined by

$$F(\boldsymbol{w}) = \int_\Omega \boldsymbol{f} \cdot \boldsymbol{w} \, \mathrm{d}V + \int_{\Gamma_{\mathrm{N}}} \boldsymbol{g} \cdot \boldsymbol{w} \, \mathrm{d}S, \tag{5}$$

and having introduced, for given $\bar{\boldsymbol{u}} \in H^{1/2}(\Gamma_{\mathrm{D}}; \mathbb{R}^3)$, the spaces $W(\bar{\boldsymbol{u}})$ and W_0 of displacement fields that are kinematically admissible with respect to arbitrary and homogeneous prescribed Dirichlet data, respectively, i.e.:

$$W(\bar{\boldsymbol{u}}) := \left\{ \boldsymbol{v} \in H^1(\Omega; \mathbb{R}^3), \, \boldsymbol{v} = \bar{\boldsymbol{u}} \text{ on } \Gamma_{\mathrm{D}} \right\}, \qquad W_0 := W(\boldsymbol{0}). \tag{6}$$

The $C^{0,\beta}(\Omega; \mathbb{R}^3)$ regularity assumption on $\boldsymbol{f}$, which is stronger than the more-usual assumption $\boldsymbol{f} \in L^2(\Omega; \mathbb{R}^3)$, ensures (e.g. from the properties of elastic volume potentials, see [31], Thm. 10.4) that $\boldsymbol{u}$ is in $C^{2,\beta}(D; \mathbb{R}^3)$ for any subset $D \Subset \Omega$. It is made in order to later permit Taylor expansions of displacements or strains about selected internal points.

2.2 Transmission problem for a small trial inhomogeneity

Now, consider a single small elastic inhomogeneity located at $\boldsymbol{z} \in \Omega$, of characteristic linear size a, occupying the domain

$$B_a = \boldsymbol{z} + a\mathcal{B},$$

where $\mathcal{B} \subset \mathbb{R}^3$ is a bounded smooth domain and a is small enough to have $\bar{B}_a \Subset \Omega$. The inhomogeneity has anisotropic properties characterized by the elasticity tensor $\boldsymbol{\mathcal{C}}^\star$, so that the elastic properties of the whole solid are defined by the tensor-valued field $\boldsymbol{\mathcal{C}}_a$ given by

$$\boldsymbol{\mathcal{C}}_a = (1 - \chi(B_a))\boldsymbol{\mathcal{C}} + \chi(B_a)\boldsymbol{\mathcal{C}}^\star = \boldsymbol{\mathcal{C}} + \chi(B_a)\Delta\boldsymbol{\mathcal{C}}, \tag{7}$$

$\chi(D)$ being the characteristic function of the domain D and $\Delta\boldsymbol{\mathcal{C}} := \boldsymbol{\mathcal{C}}^\star - \boldsymbol{\mathcal{C}}$ denoting the elastic tensor perturbation.

The displacement field $\boldsymbol{u}_a \in W(\bar{\boldsymbol{u}})$ arising in the solid containing the small inhomogeneity due to the prescribed excitations $(\boldsymbol{f}, \boldsymbol{g}, \bar{\boldsymbol{u}})$ solves the transmission problem

$$\operatorname{div}(\boldsymbol{\mathcal{C}}_a : \boldsymbol{\varepsilon}[\boldsymbol{u}_a]) + \boldsymbol{f} = \boldsymbol{0} \text{ in } \Omega, \quad (\boldsymbol{\mathcal{C}} : \boldsymbol{\varepsilon}[\boldsymbol{u}_a]) \cdot \boldsymbol{n} = \boldsymbol{g} \text{ on } \Gamma_{\mathrm{N}}, \quad \boldsymbol{u} = \bar{\boldsymbol{u}}_a \text{ on } \Gamma_{\mathrm{D}}. \tag{8}$$

Formulation (8) implicitly enforces, by virtue of its distributional interpretation, the perfect-bonding relations $\boldsymbol{u}_a|_+ = \boldsymbol{u}_a|_-$ and $(\boldsymbol{\mathcal{C}} : \boldsymbol{\varepsilon}[\boldsymbol{u}_a]) \cdot \boldsymbol{n}|_+ = (\boldsymbol{\mathcal{C}}^\star : \boldsymbol{\varepsilon}[\boldsymbol{u}_a]) \cdot \boldsymbol{n}|_-$ on ∂B_a, where the $\pm$ subscripts indicate limiting values from outside and inside B_a, respectively, and $\boldsymbol{n}$ is the unit outward normal vector to ∂B_a.

The transmission problem (8) can alternatively be formulated in terms of the displacement perturbation $\boldsymbol{v}_a := \boldsymbol{u}_a - \boldsymbol{u}$ rather than the total displacement $\boldsymbol{u}_a$. Subtracting (3) from the corresponding weak formulation of (8) yields the following weak formulation for $\boldsymbol{v}_a$:

$$\text{Find } \boldsymbol{v}_a \in W_0, \quad \langle \boldsymbol{v}_a, \boldsymbol{w} \rangle_\Omega^{\mathcal{C}_a} = -\langle \boldsymbol{u}, \boldsymbol{w} \rangle_{B_a}^{\Delta\mathcal{C}}, \quad \forall \boldsymbol{w} \in W_0. \tag{9}$$

Free-space transmission problem (FSTP). The auxiliary problem of a perfectly-bonded inhomogeneity $(\mathcal{B}, \boldsymbol{\mathcal{C}}^\star)$ embedded in an infinite elastic medium $\Omega_\infty = \mathbb{R}^3$ and subjected to a uniform remote stress equal to the background stress at $\boldsymbol{z}$ will play an important role in the sequel. The FSTP thus consists in finding the displacement field $\boldsymbol{u}_\mathcal{B}$ such that

$$\operatorname{div}(\boldsymbol{\mathcal{C}}_\mathcal{B} : \boldsymbol{\varepsilon}[\boldsymbol{u}_\mathcal{B}]) = \boldsymbol{0} \text{ in } \mathbb{R}^3, \qquad \boldsymbol{u}_\mathcal{B}(\boldsymbol{\xi}) - \boldsymbol{u}_\infty(\boldsymbol{\xi}) = O(|\boldsymbol{\xi}|^{-2}), \ |\boldsymbol{\xi}| \to \infty, \tag{10}$$

where the background displacement $\boldsymbol{u}_\infty$ is defined by $\boldsymbol{u}_\infty(\boldsymbol{\xi}) = \boldsymbol{\nabla}\boldsymbol{u}(\boldsymbol{z}) \cdot \boldsymbol{\xi}$ and with $\boldsymbol{\mathcal{C}}_\mathcal{B} := \boldsymbol{\mathcal{C}} + \chi(\mathcal{B})\Delta\boldsymbol{\mathcal{C}}$. The FSTP (10) can be recast into the following weak formulation for the displacement perturbation $\boldsymbol{v}_\mathcal{B} := \boldsymbol{u}_\mathcal{B} - \boldsymbol{u}_\infty$:

$$\text{Find } \boldsymbol{v}_\mathcal{B} \in W_\infty, \langle \boldsymbol{v}_\mathcal{B}, \boldsymbol{w} \rangle_{\mathbb{R}^3}^{\mathcal{C}_\mathcal{B}} = -\langle \boldsymbol{u}_\infty, \boldsymbol{w} \rangle_\mathcal{B}^{\Delta\mathcal{C}}, \quad \forall \boldsymbol{w} \in W_\infty, \tag{11}$$

with the function space W_∞ defined by $W_\infty = \left\{ \boldsymbol{w} \in L^2_{\mathrm{loc}}(\mathbb{R}^3; \mathbb{R}^3), \boldsymbol{\nabla}\boldsymbol{w} \in L^2(\mathbb{R}^3; \mathbb{R}^{3\times 3}) \right\}$.

When $\mathcal{B}$ is an ellipsoid, i.e. $\mathcal{B} = \{\boldsymbol{x} \in \mathbb{R}^3, \ (x_1/a_1)^2 + (x_2/a_2)^2 + (x_3/a_3)^2 \leq 1\}$, $a_1, a_2, a_3 > 0$ (with the axes of the Cartesian frame $(Ox_1x_2x_3)$ assumed, without loss of generality, to be aligned with the ellipsoid principal axes), the FSTP (12) is analytically solved in Eshelby's celebrated paper [18]. In that case, $\boldsymbol{v}_\mathcal{B}$ is found to have a constant strain and gradient inside $\mathcal{B}$, with

$$\boldsymbol{\nabla}\boldsymbol{v}_\mathcal{B}(\boldsymbol{x}) = \boldsymbol{\mathcal{S}}^{\mathrm{int}} : \boldsymbol{\varepsilon}^\star(\boldsymbol{z}), \quad \boldsymbol{\varepsilon}^\star(\boldsymbol{z}) = -(\boldsymbol{\mathcal{C}} + \Delta\boldsymbol{\mathcal{C}} : \boldsymbol{\mathcal{S}}^{\mathrm{int}})^{-1} : \Delta\boldsymbol{\mathcal{C}} : \boldsymbol{\nabla}\boldsymbol{u}(\boldsymbol{z}) \quad (\boldsymbol{x} \in \mathcal{B}), \tag{12}$$

$\boldsymbol{\mathcal{S}}^{\mathrm{int}}$ being the interior Eshelby tensor of $\mathcal{B}$, which relates a constant eigenstrain $\boldsymbol{\varepsilon}^\star$ in $\mathcal{B}$ to the constant displacement gradient in $\mathcal{B}$. We note that the above definition of $\boldsymbol{\mathcal{S}}^{\mathrm{int}}$ somewhat differs from the usual Eshelby tensor $\boldsymbol{\mathcal{S}}$, which is such that $\boldsymbol{\varepsilon}[\boldsymbol{v}_\mathcal{B}](\boldsymbol{x}) = \boldsymbol{\mathcal{S}} : \boldsymbol{\varepsilon}^\star(\boldsymbol{z})$ $(\boldsymbol{x} \in \mathcal{B})$ instead. Using e.g. Eq. (17.14) of [37], one has

$$\mathcal{S}^{\mathrm{int}}_{ijmn} = \frac{1}{4\pi} \mathcal{C}_{k\ell mn} \int_{S^2} N_{ik}(\boldsymbol{\xi}(\hat{\boldsymbol{s}})) \xi_\ell(\hat{\boldsymbol{s}}) \xi_j(\hat{\boldsymbol{s}}) \, \mathrm{d}S(\hat{\boldsymbol{s}}), \tag{13}$$

where S^2 is the unit sphere, $\boldsymbol{\xi}(\hat{\boldsymbol{s}})$ is defined for $\hat{\boldsymbol{s}} \in S^2$ by

$$\boldsymbol{\xi} = (\hat{s}_1/a_1, \hat{s}_2/a_2, \hat{s}_3/a_3), \tag{14}$$

and the tensor-valued function $\boldsymbol{\xi} \mapsto \boldsymbol{N}(\boldsymbol{\xi})$ is given by $\boldsymbol{N}(\boldsymbol{\xi}) = \boldsymbol{K}^{-1}(\boldsymbol{\xi})$, where $K_{ik}(\boldsymbol{\xi}) := \mathcal{C}_{ijk\ell}\xi_j\xi_l$ is the Christoffel acoustic tensor. A similarly modified version of the exterior Eshelby tensor will be used in Section 4.1.

Elastic moment tensor. The *elastic moment tensor* (EMT) [5, 15, 38] will be seen to play an important role in the small-inhomogeneity asymptotics of cost functionals. The EMT $\boldsymbol{\mathcal{A}}$ is the fourth-order tensor defined for any value of the constant tensor $\boldsymbol{\nabla u}(\boldsymbol{z}) \in \mathbb{R}^{3\times 3}$ by

$$\boldsymbol{\mathcal{A}} : \boldsymbol{\nabla u}(\boldsymbol{z}) = \int_{\mathcal{B}} \Delta\boldsymbol{\mathcal{C}} : \boldsymbol{\nabla u}_{\mathcal{B}} \, \mathrm{d}V = \int_{\mathcal{B}} \Delta\boldsymbol{\mathcal{C}} : (\boldsymbol{\nabla u}(\boldsymbol{z}) + \boldsymbol{\nabla v}_{\mathcal{B}}) \, \mathrm{d}V, \tag{15}$$

where $\boldsymbol{v}_{\mathcal{B}}$ is the solution of the FSTP (11). The EMT has the same symmetry properties as the elasticity tensor $\boldsymbol{\mathcal{C}}$: for any pair of second-order tensors $\boldsymbol{E}, \boldsymbol{E}' \in \mathbb{R}^{3\times 3}$, $\boldsymbol{\mathcal{A}}$ satisfies

$$\boldsymbol{E}' : \boldsymbol{\mathcal{A}} : \boldsymbol{E} = \boldsymbol{E} : \boldsymbol{\mathcal{A}} : \boldsymbol{E}' \qquad \text{(major symmetry)}, \tag{16a}$$

$$\boldsymbol{E}' : \boldsymbol{\mathcal{A}} : \boldsymbol{E} = \boldsymbol{E}' : \boldsymbol{\mathcal{A}} : \boldsymbol{E}^{\mathrm{T}} \ \text{ and } \ \boldsymbol{E}' : \boldsymbol{\mathcal{A}} : \boldsymbol{E} = \boldsymbol{E}'^{\mathrm{T}} : \boldsymbol{\mathcal{A}} : \boldsymbol{E} \qquad \text{(minor symmetries)}. \tag{16b}$$

The EMT for an ellipsoidal inhomogeneity is readily found, using (12) into (15), to have the closed form expression [5, 15, 38, 40]

$$\boldsymbol{\mathcal{A}} = |\mathcal{B}| \, \boldsymbol{\mathcal{C}} : (\boldsymbol{\mathcal{C}} + \Delta\boldsymbol{\mathcal{C}} : \boldsymbol{\mathcal{S}}^{\mathrm{int}})^{-1} : \Delta\boldsymbol{\mathcal{C}}. \tag{17}$$

Asymptotic behavior of $\boldsymbol{v}_a$ [2, 13, 15]. The inner approximation $\tilde{\boldsymbol{v}}_a$ of $\boldsymbol{v}_a$ is given by

$$\tilde{\boldsymbol{v}}_a(\boldsymbol{x}) = a\boldsymbol{v}_{\mathcal{B}}\Big(\frac{\boldsymbol{x}-\boldsymbol{z}}{a}\Big), \qquad \boldsymbol{x} \in B_a \tag{18}$$

where $\boldsymbol{v}_{\mathcal{B}}$ solves the FSTP (11). Moreover, for any cut-off function $\theta \in C_c^\infty(\Omega)$ such that $\theta \equiv 1$ in a neighborhood D of $\boldsymbol{z}$, let $\boldsymbol{\delta}_a \in H^1(\Omega; \mathbb{R}^3)$ be defined by

$$\boldsymbol{v}_a = \theta\tilde{\boldsymbol{v}}_a + \boldsymbol{\delta}_a. \tag{19}$$

Then, there exists a constant $C > 0$ independent of a such that the estimates

$$\text{(a)} \ \ \|\boldsymbol{\nabla}\tilde{\boldsymbol{v}}_a\|_{L^2(\Omega)} \le Ca^{3/2}, \quad \text{(b)} \ \ \|\tilde{\boldsymbol{v}}_a\|_{L^2(\Omega)} \le Ca^{5/2}, \quad \text{(c)} \ \ \|\boldsymbol{\delta}_a\|_{H^1(\Omega)} \le Ca^{5/2} \tag{20}$$

and

$$\text{(a)} \ \ \|\boldsymbol{\nabla}\boldsymbol{v}_a\|_{L^2(\Omega)} \le Ca^{3/2}, \quad \text{(b)} \ \ \|\boldsymbol{v}_a\|_{L^2(\Omega)} \le Ca^{5/2}. \tag{21}$$

hold [2, 15]. Estimate (20c) also relies on the previously-made assumption that $\boldsymbol{f}$ has $C^{0,\beta}$ regularity for some $\beta > 0$ in a neighbourhood of $\boldsymbol{z}$. Moreover, the known $O(|\bar{\boldsymbol{x}}|^{-3})$ far-field behavior of $\boldsymbol{\nabla v}_{\mathcal{B}}$ [15, 37] implies, by rescaling, that

$$\|\boldsymbol{\nabla}\tilde{\boldsymbol{v}}_a\|_{L^\infty(\Omega\setminus D)} \le Ca^3. \tag{22}$$

Remark 1. *As mentioned in [15], the above estimates, established assuming $\boldsymbol{\mathcal{C}}$ to be constant (homogeneous background material), are expected to also hold for heterogeneous elastic properties that are smooth in a fixed neighbourhood of $\boldsymbol{z}$ (with the EMT then defined in terms of $\boldsymbol{\mathcal{C}}(\boldsymbol{z})$). A numerical experiment involving a piecewise constant $\boldsymbol{\mathcal{C}}$ for non-destructive testing is shown in Section 5.*

2.3 Cost functional

Cost functionals of the form

$$J(\boldsymbol{\mathcal{C}}_a) = \mathbb{J}_a(\boldsymbol{u}_a, \boldsymbol{\nabla u}_a) \qquad \text{with} \quad \mathbb{J}_a(\boldsymbol{u}, \boldsymbol{d}) = \int_\Omega \psi_a\big(\boldsymbol{x}, \boldsymbol{u}(\boldsymbol{x}), \boldsymbol{d}(\boldsymbol{x})\big) \, \mathrm{d}V(\boldsymbol{x}) \tag{23}$$

are considered, where the density $\psi_a : \Omega \times \mathbb{R}^3 \times \mathbb{R}^{3\times 3} \to \mathbb{R}$ is defined by

$$\psi_a = (1 - \chi(B_a))\psi + \chi(B_a)\psi^\star = \psi + \chi(B_a)\Delta\psi, \tag{24}$$

with functions ψ and $\psi^\star$ (and hence also $\Delta\psi := \psi^\star - \psi$) assumed to be twice differentiable in all their arguments. Moreover, all second-order derivatives of ψ and $\psi^\star$ are assumed to have $C^{0,\gamma}(\Omega\times\mathbb{R}^3\times\mathbb{R}^{3\times3})$ Hölder regularity for some $\gamma>0$ with respect to all their arguments. We will denote by $\boldsymbol{x}\in\Omega$, $\boldsymbol{u}\in\mathbb{R}^3$, $\boldsymbol{d}\in\mathbb{R}^{3\times3}$ the generic arguments of a density $\psi(\boldsymbol{x},\boldsymbol{u},\boldsymbol{d})$. Then, $\partial_x\psi, \partial_u\psi, \partial_d\psi$ will denote the partial derivatives with respect to the corresponding arguments, with higher-order partial derivatives denoted similarly, e.g. $\partial^2_{ud}\psi$ (with similar notations for $\psi^\star$). The assumed Hölder regularity of ψ can thus be expressed as the existence of a finite constant K such that, for every combination of indices $i,j = x,u,d$,

$$\sup_{\substack{\boldsymbol{x}_0\in\Omega\\ \boldsymbol{u}_0\in\mathbb{R}^3\\ \boldsymbol{d}_0\in\mathbb{R}^{3\times3}}} \left|\partial^2_{ij}\psi(\boldsymbol{x}_0,\boldsymbol{u}_0,\boldsymbol{d}_0)\right| + \sup_{\substack{(\boldsymbol{x}_0,\boldsymbol{x}_1)\in\Omega\\ (\boldsymbol{u}_0,\boldsymbol{u}_1)\in\mathbb{R}^3\\ (\boldsymbol{d}_0,\boldsymbol{d}_1)\in\mathbb{R}^{3\times3}}} \frac{\left|\partial^2_{ij}\psi(\boldsymbol{x}_0,\boldsymbol{u}_0,\boldsymbol{d}_0) - \partial^2_{ij}\psi(\boldsymbol{x}_1,\boldsymbol{u}_1,\boldsymbol{d}_1)\right|}{\left(\,|\boldsymbol{x}_0-\boldsymbol{x}_1|^\gamma + |\boldsymbol{u}_0-\boldsymbol{u}_1|^\gamma + |\boldsymbol{d}_0-\boldsymbol{d}_1|^\gamma\,\right)} \le K,$$

with a similar inequality holding for $\psi^\star$. We note that the above assumption implies that $\partial^2_{ij}\psi$ and $\partial^2_{ij}\psi^\star$ are bounded over $\Omega\times\mathbb{R}^3\times\mathbb{R}^{3\times3}$.

The partial directional derivatives $\partial_u\mathbb{J}_a$ and $\partial_d\mathbb{J}_a$ of $\mathbb{J}_a$ with respect to its first and second arguments are defined, for later use, by

$$\begin{aligned}
\left\langle \partial_u\mathbb{J}_a(\boldsymbol{u},\boldsymbol{d}), \boldsymbol{w}\right\rangle &= \int_{\Omega\setminus B_a} \partial_u\psi(\boldsymbol{x},\boldsymbol{u},\boldsymbol{d})\cdot\boldsymbol{w}\,\mathrm{d}V + \int_{B_a} \partial_u\psi^\star(\boldsymbol{x},\boldsymbol{u},\boldsymbol{d})\cdot\boldsymbol{w}\,\mathrm{d}V, \quad \boldsymbol{w}\in W_0,\\
\left\langle \partial_d\mathbb{J}_a(\boldsymbol{u},\boldsymbol{d}), \boldsymbol{h}\right\rangle &= \int_{\Omega\setminus B_a} \partial_d\psi(\boldsymbol{x},\boldsymbol{u},\boldsymbol{d}):\boldsymbol{h}\,\mathrm{d}V + \int_{B_a} \partial_d\psi^\star(\boldsymbol{x},\boldsymbol{u},\boldsymbol{d}):\boldsymbol{h}\,\mathrm{d}V, \quad \boldsymbol{h}\in L^2(\Omega;\mathbb{R}^{3\times3}).
\end{aligned} \tag{25}$$

Remark 2. *The assumed Hölder and boundedness conditions on the cost functional densities might seem restrictive, but are satisfied by a number of cost functions often used in applications (compliance, energy based functionals, least squares misfit functionals, yield functions). Examples include (i) all quadratic functions of $\boldsymbol{d}$, and (ii) the useful penalization function*

$$\psi(\boldsymbol{d}) = \Psi_n(q(\boldsymbol{d})), \quad \Psi_n(t) := \left(1+t^n\right)^{1/n} - 1 \tag{26}$$

(where q is any quadratic function of $\boldsymbol{d}$), introduced in [7] to approximate pointwise yield functions with thresholds, whose derivatives Ψ_n'' and Ψ_n''' are bounded over $\mathbb{R}^+$ (one finds e.g. that $0<|\Psi_n''|\le 2^{1/n}(n-1)$ for any $t>0$, $n>1$). Case (ii) is typically used with $q(\boldsymbol{\nabla u})$ chosen as the appropriate squared (von Mises, Hill-Tsai, Drucker-Prager…) yield function, normalized so that the corresponding criterion reads $q(\boldsymbol{\nabla u})\le 1$.

3 Topological derivative

In this section, we state our main result (Theorem 1) and give its proof in Section 3.1. The generalization to piecewise-regular densities ψ is then addressed in Section 3.2. Finally, particular instances of Theorem 1 are discussed in Section 3.3.

Definition 1 (topological derivative)**.** *Assume that $J(\boldsymbol{\mathcal{C}}_a)$ can be expanded in the form*

$$J(\boldsymbol{\mathcal{C}}_a) = J(\boldsymbol{\mathcal{C}}) + \delta(a)DJ(\boldsymbol{z}) + o(\delta(a)) \tag{27}$$

where $\delta(a)$ is assumed to vanish as $a\to0$ and characterizes the small-inhomogeneity asymptotic behavior of $J(\boldsymbol{\mathcal{C}}_a)$. Then, the coefficient $DJ(\boldsymbol{z})$, which also depends a priori on the shape $\mathcal{B}$ and the moduli $\boldsymbol{\mathcal{C}},\boldsymbol{\mathcal{C}}^\star$, is called the topological derivative *of J at $\boldsymbol{z}\in\Omega$.*

Remark 3. *Terminology for the concept of topological derivative varies, with "gradient" or "sensitivity" sometimes used instead of "derivative".*

Theorem 1. *Assume a three-dimensional setting as laid out in Section 2. Any cost functional J of the form (23) and fulfilling the assumptions made in Section 2.3 admits an expansion of the form (27), with $\delta(a) = a^3$ and the topological derivative $DJ(\boldsymbol{z})$ of J at $\boldsymbol{z} \in \Omega$ given by*

$$\begin{aligned} DJ(\boldsymbol{z}) = {} & |\mathcal{B}| \Delta\psi(\boldsymbol{z}, \boldsymbol{u}(\boldsymbol{z}), \boldsymbol{\nabla u}(\boldsymbol{z})) - \boldsymbol{\nabla p}(\boldsymbol{z}) : \boldsymbol{\mathcal{A}} : \boldsymbol{\nabla u}(\boldsymbol{z}) \\ & + \partial_d(\Delta\psi)(\boldsymbol{z}, \boldsymbol{u}(\boldsymbol{z}), \boldsymbol{\nabla u}(\boldsymbol{z})) : \int_{\mathcal{B}} \boldsymbol{\nabla v}_{\mathcal{B}}(\bar{\boldsymbol{x}}) \; dV(\bar{\boldsymbol{x}}) \\ & + \int_{\mathbb{R}^3 \setminus \mathcal{B}} \mathcal{G}(\boldsymbol{z}, \boldsymbol{\nabla v}_{\mathcal{B}}(\bar{\boldsymbol{x}})) \; dV(\bar{\boldsymbol{x}}) + \int_{\mathcal{B}} \mathcal{G}^\star(\boldsymbol{z}, \boldsymbol{\nabla v}_{\mathcal{B}}(\bar{\boldsymbol{x}})) \; dV(\bar{\boldsymbol{x}}). \end{aligned} \tag{28}$$

The functions $\mathcal{G}$ and $\mathcal{G}^\star$: $\mathbb{R}^3 \times \mathbb{R}^{3\times 3} \to \mathbb{R}$ are defined, for a given background solution $\boldsymbol{u}$, by

$$\mathcal{G}(\boldsymbol{z}, \boldsymbol{d}) := \psi(\boldsymbol{z}, \boldsymbol{u}(\boldsymbol{z}), \boldsymbol{\nabla u}(\boldsymbol{z}) + \boldsymbol{d}) - \psi(\boldsymbol{z}, \boldsymbol{u}(\boldsymbol{z}), \boldsymbol{\nabla u}(\boldsymbol{z})) - \partial_d \psi(\boldsymbol{z}, \boldsymbol{u}(\boldsymbol{z}), \boldsymbol{\nabla u}(\boldsymbol{z})) : \boldsymbol{d} \tag{29a}$$

$$\mathcal{G}^\star(\boldsymbol{z}, \boldsymbol{d}) := \psi^\star(\boldsymbol{z}, \boldsymbol{u}(\boldsymbol{z}), \boldsymbol{\nabla u}(\boldsymbol{z}) + \boldsymbol{d}) - \psi^\star(\boldsymbol{z}, \boldsymbol{u}(\boldsymbol{z}), \boldsymbol{\nabla u}(\boldsymbol{z})) - \partial_d \psi^\star(\boldsymbol{z}, \boldsymbol{u}(\boldsymbol{z}), \boldsymbol{\nabla u}(\boldsymbol{z})) : \boldsymbol{d}, \tag{29b}$$

and $\boldsymbol{p} \in W_0$ is the adjoint state, defined as the solution of the weak formulation

$$\big\langle \boldsymbol{p}, \boldsymbol{w} \big\rangle_\Omega^{\mathcal{C}} = \big\langle \partial_u \mathbb{J}_0(\boldsymbol{u}, \boldsymbol{\nabla u}), \boldsymbol{w} \big\rangle + \big\langle \partial_d \mathbb{J}_0(\boldsymbol{u}, \boldsymbol{\nabla u}), \boldsymbol{\nabla w} \big\rangle \qquad \forall \boldsymbol{w} \in W_0, \tag{30}$$

with $\partial_u \mathbb{J}_0$ and $\partial_u \mathbb{J}_0$ as defined by (25).

When the densities $\psi, \psi^\star$ are linear or quadratic in their third argument (i.e. when $\partial^2_{dd}\psi$ and $\partial^2_{dd}\psi^\star$ are independent on $\boldsymbol{d}$), letting $\boldsymbol{\mathcal{D}}(\boldsymbol{z}) := \partial^2_{dd}\psi(\boldsymbol{z}, \boldsymbol{u}(\boldsymbol{z}))$ and $\boldsymbol{\mathcal{D}}^\star(\boldsymbol{z}) := \partial^2_{dd}\psi^\star(\boldsymbol{z}, \boldsymbol{u}(\boldsymbol{z}))$, the last two terms in (28) are given by the more explicit expression

$$\frac{1}{2} \int_{\mathbb{R}^3 \setminus \mathcal{B}} \boldsymbol{\nabla v}_{\mathcal{B}}(\bar{\boldsymbol{x}}) : \boldsymbol{\mathcal{D}}(\boldsymbol{z}) : \boldsymbol{\nabla v}_{\mathcal{B}}(\bar{\boldsymbol{x}}) \; dV(\bar{\boldsymbol{x}}) + \frac{1}{2} \int_{\mathcal{B}} \boldsymbol{\nabla v}_{\mathcal{B}}(\bar{\boldsymbol{x}}) : \boldsymbol{\mathcal{D}}^\star(\boldsymbol{z}) : \boldsymbol{\nabla v}_{\mathcal{B}}(\bar{\boldsymbol{x}}) \; dV(\bar{\boldsymbol{x}})$$

Moreover, under two-dimensional plane-strain conditions (where only in-plane displacements are nonzero), the result (28) still holds (with $\Omega \subset \mathbb{R}^2$, $\mathcal{B} \subset \mathbb{R}^2$ and the next-to-last integral now taken over $\mathbb{R}^2 \setminus \mathcal{B}$), while $\delta(a) = a^2$ in expansion (27).

Remark 4. *The result (28) for DJ involves the gradient $\boldsymbol{\nabla v}_{\mathcal{B}}$ of the FSTP solution, rather than just its strain $\boldsymbol{\varepsilon}[\boldsymbol{v}_{\mathcal{B}}]$, which explains the definition (10) chosen here for the Eshelby tensor.*

3.1 Proof of Theorem 1

The detailed proof to follow concentrates on the 3D case, its adaptation to the 2D case being then outlined in a comment. The proof consists in finding the leading contribution to the difference $J(\boldsymbol{\mathcal{C}}_a) - J(\boldsymbol{\mathcal{C}}) = \mathbb{J}_a(\boldsymbol{u}_a, \boldsymbol{\nabla u}_a) - \mathbb{J}_0(\boldsymbol{u}, \boldsymbol{\nabla u})$ as $a \to 0$. To this end, we write

$$\begin{aligned} \mathbb{J}_a(\boldsymbol{u}_a, \boldsymbol{\nabla u}_a) - \mathbb{J}_0(\boldsymbol{u}, \boldsymbol{\nabla u}) = {} & \Big(\mathbb{J}_a(\boldsymbol{u}, \boldsymbol{\nabla u}) - \mathbb{J}_0(\boldsymbol{u}, \boldsymbol{\nabla u}) \Big) \\ & + \Big(\mathbb{J}_a(\boldsymbol{u}_a, \boldsymbol{\nabla u}_a) - \mathbb{J}_a(\boldsymbol{u}, \boldsymbol{\nabla u}_a) - \big\langle \partial_u \mathbb{J}_a(\boldsymbol{u}, \boldsymbol{\nabla u}), \boldsymbol{v}_a \big\rangle \Big) \\ & + \Big(\mathbb{J}_a(\boldsymbol{u}, \boldsymbol{\nabla u}_a) - \mathbb{J}_a(\boldsymbol{u}, \boldsymbol{\nabla u}) - \big\langle \partial_d \mathbb{J}_a(\boldsymbol{u}, \boldsymbol{\nabla u}), \boldsymbol{\nabla v}_a \big\rangle \Big) \\ & + \Big(\big\langle \partial_u \mathbb{J}_a(\boldsymbol{u}, \boldsymbol{\nabla u}), \boldsymbol{v}_a \big\rangle + \big\langle \partial_d \mathbb{J}_a(\boldsymbol{u}, \boldsymbol{\nabla u}), \boldsymbol{\nabla v}_a \big\rangle \Big), \end{aligned} \tag{31}$$

with $\partial_u \mathbb{J}_a$ and $\partial_u \mathbb{J}_a$ as defined by (25), and separately evaluate the leading contribution of each bracketed term in the right-hand side of (31); this is done in the following Lemmas 2 to 5. Using the results of the lemmas in the above decomposition then directly establishes both the expansion (27) and the expression (28) of $\mathrm{D}J(\boldsymbol{z})$ stated in Theorem 1.

Lemma 2. *Let $\Delta\psi$ be defined as in* (24)*. One has*

$$\mathbb{J}_a(\boldsymbol{u}, \boldsymbol{\nabla u}) - \mathbb{J}_0(\boldsymbol{u}, \boldsymbol{\nabla u}) = a^3 |\mathcal{B}| \Delta\psi(\boldsymbol{z}, \boldsymbol{u}(\boldsymbol{z}), \boldsymbol{\nabla u}(\boldsymbol{z})) + o(a^3).$$

Proof. By interior regularity for $\boldsymbol{u}$ and the assumed smoothness of $\psi, \psi^\star$, $\Delta\psi(\boldsymbol{x}, \boldsymbol{u}(\boldsymbol{x}), \boldsymbol{\nabla u}(\boldsymbol{x}))$ is continuous at $\boldsymbol{x} = \boldsymbol{z}$. Therefore, the Lemma follows easily from:

$$\begin{aligned}\mathbb{J}_a(\boldsymbol{u}, \boldsymbol{\nabla u}) - \mathbb{J}_0(\boldsymbol{u}, \boldsymbol{\nabla u}) &= \int_\Omega \big(\psi_a(\boldsymbol{x}, \boldsymbol{u}, \boldsymbol{\nabla u}) - \psi(\boldsymbol{x}, \boldsymbol{u}, \boldsymbol{\nabla u})\big)\, \mathrm{d}V(\boldsymbol{x}) \\ &= \int_{B_a} \Delta\psi(\boldsymbol{x}, \boldsymbol{u}, \boldsymbol{\nabla u})\, \mathrm{d}V(\boldsymbol{x}) = a^3 |\mathcal{B}| \Delta\psi(\boldsymbol{z}, \boldsymbol{u}(\boldsymbol{z}), \boldsymbol{\nabla u}(\boldsymbol{z})) + o(a^3),\end{aligned}$$

where the last step exploits the fact that the volume of B_a is $|B_a| = a^3|\mathcal{B}|$. □

Lemma 3. *Let the displacement perturbation $\boldsymbol{v}_a$ solve problem* (9)*. One has*

$$\mathbb{J}_a(\boldsymbol{u}_a, \boldsymbol{\nabla u}_a) - \mathbb{J}_a(\boldsymbol{u}, \boldsymbol{\nabla u}_a) - \big\langle \partial_u \mathbb{J}_a(\boldsymbol{u}, \boldsymbol{\nabla u}), \boldsymbol{v}_a \big\rangle = o(a^3),$$

with $\partial_u \mathbb{J}_a$ as defined by (25)

Proof. The proof is based on Taylor expansions. A first-order expansion of ψ with respect to its first argument first yields

$$\psi(\boldsymbol{x}, \boldsymbol{u}_a, \boldsymbol{\nabla u}_a) - \psi(\boldsymbol{x}, \boldsymbol{u}, \boldsymbol{\nabla u}_a) = \partial_u \psi(\boldsymbol{x}, \boldsymbol{u}, \boldsymbol{\nabla u}_a) \cdot \boldsymbol{v}_a + \tfrac{1}{2} \boldsymbol{v}_a \cdot \partial^2_{uu} \psi(\boldsymbol{x}, \boldsymbol{u} + \delta_u \boldsymbol{v}_a, \boldsymbol{\nabla u}_a) \cdot \boldsymbol{v}_a$$

for some $\delta_u(\boldsymbol{x}) \in [0, 1]$. Moreover, a zeroth-order Taylor expansion of $\partial_u \psi$ with respect to its second argument gives

$$\partial_u \psi(\boldsymbol{x}, \boldsymbol{u}, \boldsymbol{\nabla u}_a) \cdot \boldsymbol{v}_a - \partial_u \psi(\boldsymbol{x}, \boldsymbol{u}, \boldsymbol{\nabla u}) \cdot \boldsymbol{v}_a = \boldsymbol{\nabla v}_a : \partial^2_{du} \psi(\boldsymbol{x}, \boldsymbol{u}, \boldsymbol{\nabla u} + \delta_d \boldsymbol{\nabla v}_a) \cdot \boldsymbol{v}_a$$

for some $\delta_d(\boldsymbol{x}) \in [0, 1]$. Both expansions are valid due to the assumed regularity of ψ. Similar expansions also hold for the density $\psi^\star$, for some $\delta^\star_u(\boldsymbol{x}), \delta^\star_d(\boldsymbol{x}) \in [0, 1]$. Combining all of these expansions, one finds

$$\mathbb{J}_a(\boldsymbol{u}_a, \boldsymbol{\nabla u}_a) - \mathbb{J}_a(\boldsymbol{u}, \boldsymbol{\nabla u}_a) = \big\langle \partial_u \mathbb{J}_a(\boldsymbol{u}, \boldsymbol{\nabla u}), \boldsymbol{v}_a \big\rangle + R_a \tag{32}$$

with the remainder R_a given by

$$\begin{aligned}R_a = &\int_{\Omega \setminus B_a} \Big[\tfrac{1}{2} \boldsymbol{v}_a \cdot \partial^2_{uu} \psi(\boldsymbol{x}, \boldsymbol{u} + \delta_u \boldsymbol{v}_a, \boldsymbol{\nabla u}_a) \cdot \boldsymbol{v}_a + \boldsymbol{\nabla v}_a : \partial^2_{du} \psi(\boldsymbol{x}, \boldsymbol{u}, \boldsymbol{\nabla u} + \delta_d \boldsymbol{\nabla v}_a) \cdot \boldsymbol{v}_a \Big]\, \mathrm{d}V \\ &+ \int_{B_a} \Big[\tfrac{1}{2} \boldsymbol{v}_a \cdot \partial^2_{uu} \psi^\star(\boldsymbol{x}, \boldsymbol{u} + \delta^\star_u \boldsymbol{v}_a, \boldsymbol{\nabla u}_a) \cdot \boldsymbol{v}_a + \boldsymbol{\nabla v}_a : \partial^2_{du} \psi^\star(\boldsymbol{x}, \boldsymbol{u}, \boldsymbol{\nabla u} + \delta^\star_d \boldsymbol{\nabla v}_a) \cdot \boldsymbol{v}_a \Big]\, \mathrm{d}V\end{aligned}$$

Next, thanks to the boundedness of the second-order partial derivatives of ψ and $\psi^\star$, there exists a constant $C > 0$ such that

$$R_a \leq C(\|\boldsymbol{v}_a\|^2_{L^2(\Omega)} + \|\boldsymbol{\nabla v}_a\|_{L^2(\Omega)} \|\boldsymbol{v}_a\|_{L^2(\Omega)})$$

Finally, estimates (21) imply that there exists a constant $C > 0$ such that

$$R_a \leq C a^4 = o(a^3).$$

Using the above estimate in (32) completes the proof. □

Lemma 4. *One has*

$$\begin{aligned}\mathbb{J}_a(\boldsymbol{u},\boldsymbol{\nabla u}_a)-\mathbb{J}_a(\boldsymbol{u},\boldsymbol{\nabla u})-\big\langle\partial_d\mathbb{J}_a(\boldsymbol{u},\boldsymbol{\nabla u}),\boldsymbol{\nabla v}_a\big\rangle\\ =a^3\Big\{\int_{\mathbb{R}^3\setminus\mathcal{B}}\mathcal{G}(\boldsymbol{z},\boldsymbol{\nabla v}_{\mathcal{B}}(\bar{\boldsymbol{x}}))\;dV(\bar{\boldsymbol{x}})+\int_{\mathcal{B}}\mathcal{G}^\star(\boldsymbol{z},\boldsymbol{\nabla v}_{\mathcal{B}}(\bar{\boldsymbol{x}}))\;dV(\bar{\boldsymbol{x}})\Big\}+o(a^3)\end{aligned}\tag{33}$$

where $\partial_d\mathbb{J}_a$ is defined by (25) *and the functions $\mathcal{G}$ and $\mathcal{G}^\star$: $\mathbb{R}^3\times\mathbb{R}^{3\times3}\to\mathbb{R}$ are defined by (29a,b).*

Proof. The combination to be estimated is first recast in the form

$$\begin{aligned}&\mathbb{J}_a(\boldsymbol{u},\boldsymbol{\nabla u}_a)-\mathbb{J}_a(\boldsymbol{u},\boldsymbol{\nabla u})-\big\langle\partial_d\mathbb{J}_a(\boldsymbol{u},\boldsymbol{\nabla u}),\boldsymbol{\nabla v}_a\big\rangle\\ &\quad=\int_{\Omega\setminus B_a}\mathcal{G}(\boldsymbol{x},\boldsymbol{\nabla v}_a)\,\mathrm{d}V(\boldsymbol{x})+\int_{B_a}\mathcal{G}^\star(\boldsymbol{x},\boldsymbol{\nabla v}_a)\,\mathrm{d}V(\boldsymbol{x})\\ &\quad=\Big(\mathbb{J}_a(\boldsymbol{u},\boldsymbol{\nabla u}_a)-\mathbb{J}_a(\boldsymbol{u},\boldsymbol{\nabla u}+\boldsymbol{\nabla}\tilde{\boldsymbol{v}}_a)-\big\langle\partial_d\mathbb{J}_a(\boldsymbol{u},\boldsymbol{\nabla u}+\boldsymbol{\nabla}\tilde{\boldsymbol{v}}_a),\boldsymbol{\nabla}\hat{\boldsymbol{v}}_a\big\rangle\Big)\\ &\qquad+\Big(\partial_d\mathbb{J}_a(\boldsymbol{u},\boldsymbol{\nabla u}+\boldsymbol{\nabla}\tilde{\boldsymbol{v}}_a),\boldsymbol{\nabla}\hat{\boldsymbol{v}}_a\big\rangle-\big\langle\partial_d\mathbb{J}_a(\boldsymbol{u},\boldsymbol{\nabla u}),\boldsymbol{\nabla}\hat{\boldsymbol{v}}_a\big\rangle\Big)\\ &\qquad+\Big(\mathbb{J}_a(\boldsymbol{u},\boldsymbol{\nabla u}+\boldsymbol{\nabla}\tilde{\boldsymbol{v}}_a)-\mathbb{J}_a(\boldsymbol{u},\boldsymbol{\nabla u})-\big\langle\partial_d\mathbb{J}_a(\boldsymbol{u},\boldsymbol{\nabla u}),\boldsymbol{\nabla}\tilde{\boldsymbol{v}}_a\big\rangle\Big)\end{aligned}\tag{34a}$$

having used functions $\mathcal{G}$, $\mathcal{G}^\star$ defined by (29a,b) for the last equality, and with $\hat{\boldsymbol{v}}_a$ defined (using (19) in the second equality below) by

$$\hat{\boldsymbol{v}}_a=\boldsymbol{v}_a-\tilde{\boldsymbol{v}}_a=\boldsymbol{\delta}_a+(\theta-1)\tilde{\boldsymbol{v}}_a.\tag{34b}$$

Since $\boldsymbol{\nabla}\hat{\boldsymbol{v}}_a=\boldsymbol{\nabla}\boldsymbol{\delta}_a+(\theta-1)\boldsymbol{\nabla}\tilde{\boldsymbol{v}}_a+\boldsymbol{\nabla}\theta\otimes\tilde{\boldsymbol{v}}_a$, we note for later use that estimates (20) and (22) (together with the fact that the support of $(\theta-1)\boldsymbol{\nabla}\tilde{\boldsymbol{v}}_a$ is $\Omega\setminus D$) imply

$$\|\boldsymbol{\nabla}\hat{\boldsymbol{v}}_a\|_{L^2(\Omega)}=O(a^{5/2}).\tag{34c}$$

We first focus on contributions of integrals over $\Omega\setminus B_a$, i.e. of the density $\mathcal{G}$, to (34a). To begin, each bracketed combination in (34a) is reformulated by exploiting Taylor expansions (of first-order with respect to its third argument, with integral remainder) of ψ, to obtain

$$\begin{aligned}\int_{\Omega\setminus B_a}\mathcal{G}(\boldsymbol{x},\boldsymbol{\nabla v}_a)\,\mathrm{d}V(\boldsymbol{x})=&\int_{\Omega\setminus B_a}\boldsymbol{\nabla}\hat{\boldsymbol{v}}_a(\boldsymbol{x}):\boldsymbol{D}_2\big(\boldsymbol{x},\boldsymbol{u}+\tilde{\boldsymbol{v}}_a,\boldsymbol{\nabla}\hat{\boldsymbol{v}}_a(\boldsymbol{x})\big):\boldsymbol{\nabla}\hat{\boldsymbol{v}}_a(\boldsymbol{x})\,\mathrm{d}V(\boldsymbol{x})\\ &+\int_{\Omega\setminus B_a}\boldsymbol{\nabla}\hat{\boldsymbol{v}}_a(\boldsymbol{x}):\boldsymbol{D}_1\big(\boldsymbol{x},\boldsymbol{\nabla}\hat{\boldsymbol{v}}_a(\boldsymbol{x})\big):\boldsymbol{\nabla}\tilde{\boldsymbol{v}}_a(\boldsymbol{x})\,\mathrm{d}V(\boldsymbol{x})\\ &+\int_{\Omega\setminus B_a}\boldsymbol{\nabla}\tilde{\boldsymbol{v}}_a(\boldsymbol{x}):\boldsymbol{D}_3\big(\boldsymbol{x},\boldsymbol{\nabla}\tilde{\boldsymbol{v}}_a(\boldsymbol{x})\big):\boldsymbol{\nabla}\tilde{\boldsymbol{v}}_a(\boldsymbol{x})\,\mathrm{d}V(\boldsymbol{x}),\end{aligned}\tag{34d}$$

with

$$\begin{aligned}\boldsymbol{D}_1(\boldsymbol{y},\boldsymbol{d})&=\int_0^1\partial_{dd}\psi\big(\,\boldsymbol{y},\boldsymbol{u}(\boldsymbol{y}),\boldsymbol{\nabla u}(\boldsymbol{y})+t\boldsymbol{d})\,\big)\,\mathrm{d}t,\\ \boldsymbol{D}_2(\boldsymbol{y},\boldsymbol{w},\boldsymbol{d})&=\int_0^1\partial_{dd}\psi\big(\,\boldsymbol{y},\boldsymbol{u}(\boldsymbol{y}),\boldsymbol{\nabla w}(\boldsymbol{y})+t\boldsymbol{d}\,\big)\,(1-t)\,\mathrm{d}t,\\ \boldsymbol{D}_3(\boldsymbol{y},\boldsymbol{d})&=\boldsymbol{D}_2(\boldsymbol{y},\boldsymbol{u},\boldsymbol{d}).\end{aligned}\tag{34e}$$

Both $\boldsymbol{D}_1\big(\boldsymbol{x}, \boldsymbol{\nabla}\hat{\boldsymbol{v}}_a(\boldsymbol{x})\big)$ and $\boldsymbol{D}_2\big(\boldsymbol{x}, \boldsymbol{u}(\boldsymbol{x})+\tilde{\boldsymbol{v}}_a(\boldsymbol{x}), \boldsymbol{\nabla}\hat{\boldsymbol{v}}_a(\boldsymbol{x})\big)$ are bounded over Ω, due to the boundedness of the second-order partial derivatives of ψ. This remark is exploited by applying the Cauchy-Schwarz inequality to the first two integrals I_1 and I_2 of the right-hand side of (34d) and invoking estimates (20a) and (34c), to obtain $I_1 = O(a^5) = o(a^3)$ and $I_2 = O(a^4) = o(a^3)$. Using these estimates, applying the change of variables $\bar{\boldsymbol{x}} = (\boldsymbol{x}-\boldsymbol{z})/a$ to the third integral of the right-hand side of (34d) (whereby $\mathrm{d}V(\boldsymbol{x}) = a^3\,\mathrm{d}V(\bar{\boldsymbol{x}})$), and recalling definition (19) of $\tilde{\boldsymbol{v}}_a$, we obtain

$$\begin{aligned}\int_{\Omega\setminus B_a} \mathcal{G}(\boldsymbol{x}, \boldsymbol{\nabla}\tilde{\boldsymbol{v}}_a)\,\mathrm{d}V(\boldsymbol{x}) &= a^3 \int_{((\Omega-\boldsymbol{z})/a)\setminus\mathcal{B}} \boldsymbol{\nabla}\boldsymbol{v}_{\mathcal{B}}(\bar{\boldsymbol{x}}) : \boldsymbol{D}_3(\boldsymbol{z}+a\bar{\boldsymbol{x}}, \boldsymbol{\nabla}\boldsymbol{v}_{\mathcal{B}}(\bar{\boldsymbol{x}})) : \boldsymbol{\nabla}\boldsymbol{v}_{\mathcal{B}}(\bar{\boldsymbol{x}})\,\mathrm{d}V(\bar{\boldsymbol{x}}) + o(a^3)\\ &= a^3 \int_{((\Omega-\boldsymbol{z})/a)\setminus\mathcal{B}} \boldsymbol{\nabla}\boldsymbol{v}_{\mathcal{B}}(\bar{\boldsymbol{x}}) : \boldsymbol{D}_3(\boldsymbol{z}, \boldsymbol{\nabla}\boldsymbol{v}_{\mathcal{B}}(\bar{\boldsymbol{x}})) : \boldsymbol{\nabla}\boldsymbol{v}_{\mathcal{B}}(\bar{\boldsymbol{x}})\,\mathrm{d}V(\bar{\boldsymbol{x}}) + R + o(a^3)\\ &= a^3 \int_{((\Omega-\boldsymbol{z})/a)\setminus\mathcal{B}} \mathcal{G}(\boldsymbol{z}, \boldsymbol{\nabla}\boldsymbol{v}_{\mathcal{B}}(\bar{\boldsymbol{x}}))\,\mathrm{d}V(\bar{\boldsymbol{x}}) + R + o(a^3) \qquad (34f)\end{aligned}$$

(having noted that $\boldsymbol{\nabla}\boldsymbol{v}_{\mathcal{B}}(\bar{\boldsymbol{x}}) : \boldsymbol{D}_3(\boldsymbol{z}, \boldsymbol{\nabla}\boldsymbol{v}_{\mathcal{B}}(\bar{\boldsymbol{x}})) : \boldsymbol{\nabla}\boldsymbol{v}_{\mathcal{B}}(\bar{\boldsymbol{x}}) = \mathcal{G}(\boldsymbol{z}, \boldsymbol{\nabla}\boldsymbol{v}_{\mathcal{B}}(\bar{\boldsymbol{x}}))$), where the remainder R is such that

$$\begin{aligned}R &:= a^3 \int_{((\Omega-\boldsymbol{z})/a)\setminus\mathcal{B}} \boldsymbol{\nabla}\boldsymbol{v}_{\mathcal{B}}(\bar{\boldsymbol{x}}) : \big[\boldsymbol{D}_3(\boldsymbol{z}+a\bar{\boldsymbol{x}}, \boldsymbol{\nabla}\boldsymbol{v}_{\mathcal{B}}(\bar{\boldsymbol{x}})) - \boldsymbol{D}_3(\boldsymbol{z}, \boldsymbol{\nabla}\boldsymbol{v}_{\mathcal{B}}(\bar{\boldsymbol{x}}))\big] : \boldsymbol{\nabla}\boldsymbol{v}_{\mathcal{B}}(\bar{\boldsymbol{x}})\,\mathrm{d}V(\bar{\boldsymbol{x}})\\ &\le Ca^{3+\gamma} \int_{((\Omega-\boldsymbol{z})/a)\setminus\mathcal{B}} |\boldsymbol{\nabla}\boldsymbol{v}_{\mathcal{B}}(\bar{\boldsymbol{x}})|^2 |\bar{\boldsymbol{x}}|^\gamma\,\mathrm{d}V(\bar{\boldsymbol{x}}) \le Ca^{3+\gamma} \int_{\mathbb{R}^3\setminus\mathcal{B}} |\boldsymbol{\nabla}\boldsymbol{v}_{\mathcal{B}}(\bar{\boldsymbol{x}})|^2 |\bar{\boldsymbol{x}}|^\gamma\,\mathrm{d}V(\bar{\boldsymbol{x}}), \qquad (34g)\end{aligned}$$

by virtue of the inequality

$$|\boldsymbol{D}_3(\boldsymbol{z}+a\bar{\boldsymbol{x}}, \boldsymbol{d}) - \boldsymbol{D}_3(\boldsymbol{z}, \boldsymbol{d})| \le Ca^\gamma |\bar{\boldsymbol{x}}|^\gamma \qquad (34h)$$

stemming from the assumed $C^{0,\gamma}$ Hölder regularity of $\partial_{dd}\psi$ and the known C^2 interior regularity of $\boldsymbol{u}$ in Ω, which implies that there exists $\tau', \tau'' \in [0,1]$ such that

$$\boldsymbol{u}(\boldsymbol{x}) - \boldsymbol{u}(\boldsymbol{z}) = a\boldsymbol{\nabla}\boldsymbol{u}(\boldsymbol{z}+\tau' a\bar{\boldsymbol{x}})\cdot\bar{\boldsymbol{x}}, \qquad \boldsymbol{\nabla}\boldsymbol{u}(\boldsymbol{x}) - \boldsymbol{\nabla}\boldsymbol{u}(\boldsymbol{z}) = a\boldsymbol{\nabla}^2\boldsymbol{u}(\boldsymbol{z}+\tau'' a\bar{\boldsymbol{x}})\cdot\bar{\boldsymbol{x}}. \qquad (34i)$$

The known $O(|\bar{\boldsymbol{x}}|^{-3})$ far-field behavior of $\boldsymbol{\nabla}\boldsymbol{v}_{\mathcal{B}}(\bar{\boldsymbol{x}})$ [15, 37] implies that the last integral in (34g) over the unbounded domain $\mathbb{R}^3\setminus\mathcal{B}$ is finite for any $\gamma < 3$, and hence that $R = O(a^{3+\gamma}) = o(a^3)$. Finally, taking the limit $((\Omega-\boldsymbol{z})/a)\setminus\mathcal{B} \to \mathbb{R}^3\setminus\mathcal{B}$ in (34f) (which is legitimate by the dominated convergence theorem since $|\mathcal{G}(\boldsymbol{z}, \boldsymbol{\nabla}\boldsymbol{v}_{\mathcal{B}}(\bar{\boldsymbol{x}}))|$ is integrable over $\mathbb{R}^3 \setminus \mathcal{B}$), the desired asymptotic form of (34d) is obtained:

$$\int_{\Omega\setminus B_a} \mathcal{G}(\boldsymbol{x}, \boldsymbol{\nabla}\boldsymbol{v}_a)\,\mathrm{d}V(\boldsymbol{x}) = a^3 \int_{\mathbb{R}^3\setminus\mathcal{B}} \mathcal{G}(\boldsymbol{z}, \boldsymbol{\nabla}\boldsymbol{v}_{\mathcal{B}}(\bar{\boldsymbol{x}}))\,\mathrm{d}V(\bar{\boldsymbol{x}}) + o(a^3). \qquad (34j)$$

The second integral in the right-hand side of (34a) can be estimated following similar arguments. A representation similar to (34d) holds, with integrals taken over B_a and ψ replaced by $\psi^\star$ in (34e). Noting in addition that now $\hat{\boldsymbol{v}}_a = \boldsymbol{\delta}_a$ since $\theta = 1$ in B_a, the first two integrals in the right-hand side of the counterpart of (34d) are easily established to be of order $o(a^3)$ using estimates (20). Using again the change of variables $\bar{\boldsymbol{x}} = (\boldsymbol{x}-\boldsymbol{z})/a$ in the remaining integral, one then finds

$$\int_{B_a} \mathcal{G}^\star(\boldsymbol{x}, \boldsymbol{\nabla}\boldsymbol{v}_a)\,\mathrm{d}V(\boldsymbol{x}) = a^3 \int_{\mathcal{B}} \mathcal{G}^\star(\boldsymbol{z}, \boldsymbol{\nabla}\boldsymbol{v}_{\mathcal{B}}(\bar{\boldsymbol{x}}))\,\mathrm{d}V(\bar{\boldsymbol{x}}) + R^\star + o(a^3), \qquad (34k)$$

where, exploiting through (34h) the assumed Hölder regularity of $\psi^\star$, the remainder $R^\star$ is such that

$$R^\star := a^3 \int_{\mathcal{B}} \boldsymbol{\nabla v}_{\mathcal{B}}(\bar{\boldsymbol{x}}) : \big[\boldsymbol{D}(\boldsymbol{z}+a\bar{\boldsymbol{x}}, \boldsymbol{\nabla v}_{\mathcal{B}}(\bar{\boldsymbol{x}})) - \boldsymbol{D}(\boldsymbol{z}, \boldsymbol{\nabla v}_{\mathcal{B}}(\bar{\boldsymbol{x}}))\big] : \boldsymbol{\nabla v}_{\mathcal{B}}(\bar{\boldsymbol{x}}) \, \mathrm{d}V(\bar{\boldsymbol{x}}) \\ \leq Ca^{3+\gamma} \int_{\mathcal{B}} |\boldsymbol{\nabla v}_{\mathcal{B}}(\bar{\boldsymbol{x}})|^2 |\bar{\boldsymbol{x}}|^\gamma \, \mathrm{d}V(\bar{\boldsymbol{x}}) = O(a^{3+\gamma}).$$

The desired asymptotic form of (34k) is therefore obtained:

$$\int_{B_a} \mathcal{G}^\star(\boldsymbol{x}, \boldsymbol{\nabla v}_a) \, \mathrm{d}V(\boldsymbol{x}) = a^3 \int_{\mathcal{B}} \mathcal{G}^\star(\boldsymbol{z}, \boldsymbol{\nabla v}_{\mathcal{B}}(\bar{\boldsymbol{x}})) \, \mathrm{d}V(\bar{\boldsymbol{x}}) + o(a^3) \tag{34l}$$

The lemma finally follows from using expansions (34j) and (34l) in (34a). □

Finally, the leading contribution to the last bracketed combination of (31) is given in the following lemma in terms of an adjoint solution.

Lemma 5. *Let the adjoint solution $\boldsymbol{p} \in W_0$ be defined by the weak formulation*

$$\big\langle \boldsymbol{p}, \boldsymbol{w} \big\rangle_\Omega^{\mathcal{C}} = \big\langle \partial_u \mathbb{J}_0(\boldsymbol{u}, \boldsymbol{\nabla u}), \boldsymbol{w} \big\rangle + \big\langle \partial_d \mathbb{J}_0(\boldsymbol{u}, \boldsymbol{\nabla u}), \boldsymbol{\nabla w} \big\rangle \qquad \forall \boldsymbol{w} \in W_0, \tag{35}$$

with $\partial_u \mathbb{J}_0$ and $\partial_d \mathbb{J}_0$ as defined by (25)*. One has*

$$\big\langle \partial_u \mathbb{J}_a(\boldsymbol{u}, \boldsymbol{\nabla u}), \boldsymbol{v}_a \big\rangle + \big\langle \partial_d \mathbb{J}_a(\boldsymbol{u}, \boldsymbol{\nabla u}), \boldsymbol{\nabla v}_a \big\rangle \\ = a^3 |\mathcal{B}| \Big\{ - \boldsymbol{\nabla p}(\boldsymbol{z}) : \boldsymbol{\mathcal{A}} : \boldsymbol{\nabla u}(\boldsymbol{z}) + \partial_d(\Delta\psi)(\boldsymbol{z}, \boldsymbol{u}(\boldsymbol{z}), \boldsymbol{\nabla u}(\boldsymbol{z})) : \int_{\mathcal{B}} \boldsymbol{\nabla v}_{\mathcal{B}} \, dV(\bar{\boldsymbol{x}}) \Big\} + o(a^3) \tag{36}$$

Proof. Setting $\Delta\psi := \psi^\star - \psi$, one has

$$\big\langle \partial_u \mathbb{J}_a(\boldsymbol{u}, \boldsymbol{\nabla u}), \boldsymbol{v}_a \big\rangle + \big\langle \partial_d \mathbb{J}_a(\boldsymbol{u}, \boldsymbol{\nabla u}), \boldsymbol{\nabla v}_a \big\rangle = \big\langle \partial_u \mathbb{J}_0(\boldsymbol{u}, \boldsymbol{\nabla u}), \boldsymbol{v}_a \big\rangle + \big\langle \partial_d \mathbb{J}_0(\boldsymbol{u}, \boldsymbol{\nabla u}), \boldsymbol{\nabla v}_a \big\rangle \\ + \big\langle \partial_u \Delta\mathbb{J}(\boldsymbol{u}, \boldsymbol{\nabla u}), \boldsymbol{v}_a \big\rangle + \big\langle \partial_d \Delta\mathbb{J}(\boldsymbol{u}, \boldsymbol{\nabla u}), \boldsymbol{\nabla v}_a \big\rangle \tag{37a}$$

Invoking the definition (35) of the adjoint solution, the identity

$$\big\langle \boldsymbol{v}_a, \boldsymbol{w} \big\rangle_\Omega^{\mathcal{C}} = -\big\langle \boldsymbol{u}_a, \boldsymbol{w} \big\rangle_{B_a}^{\Delta\mathcal{C}}, \quad \forall \boldsymbol{w} \in W_0$$

verified by the transmission problem, one finds

$$\big\langle \partial_u \mathbb{J}_0(\boldsymbol{u}, \boldsymbol{\nabla u}), \boldsymbol{v}_a \big\rangle + \big\langle \partial_d \mathbb{J}_0(\boldsymbol{u}, \boldsymbol{\nabla u}), \boldsymbol{\nabla v}_a \big\rangle = \big\langle \boldsymbol{p}, \boldsymbol{v}_a \big\rangle_\Omega^{\mathcal{C}} = -\big\langle \boldsymbol{u}_a, \boldsymbol{p} \big\rangle_{B_a}^{\Delta\mathcal{C}} \\ = -a^3 |\mathcal{B}| \boldsymbol{\nabla p}(\boldsymbol{z}) : \boldsymbol{\mathcal{A}} : \boldsymbol{\nabla u}(\boldsymbol{z}) + o(a^3), \tag{37b}$$

where the last equality holds by virtue of [15, Lemma 2] and $\boldsymbol{p}$ having C^2 interior regularity (see Section 3.2). Next, using decomposition (19) of $\boldsymbol{v}_a$ and the fact that $\Delta\mathbb{J}$ has B_a as its geometrical support (implying in particular that $\theta = 1$ in B_a), one has

$$\big\langle \partial_u \Delta\mathbb{J}(\boldsymbol{u}, \boldsymbol{\nabla u}), \boldsymbol{v}_a \big\rangle + \big\langle \partial_d \Delta\mathbb{J}(\boldsymbol{u}, \boldsymbol{\nabla u}), \boldsymbol{\nabla v}_a \big\rangle \\ = \big\langle \partial_u \Delta\mathbb{J}(\boldsymbol{u}, \boldsymbol{\nabla u}), (\tilde{\boldsymbol{v}}_a + \boldsymbol{\delta}_a) \big\rangle + \big\langle \partial_d \Delta\mathbb{J}(\boldsymbol{u}, \boldsymbol{\nabla u}), \boldsymbol{\nabla}(\tilde{\boldsymbol{v}}_a + \boldsymbol{\delta}_a) \big\rangle \tag{37c}$$

The partial derivatives of $\Delta\psi(\boldsymbol{x}, \boldsymbol{u}(\boldsymbol{x}), \boldsymbol{\nabla u}(\boldsymbol{x}))$ being bounded by virtue of the assumptions made on ψ, $\psi^\star$ and the C^2 interior regularity of $\boldsymbol{u}$, there exists a constant $C > 0$ such that

$$\big\langle \partial_u \Delta\mathbb{J}(\boldsymbol{u}, \boldsymbol{\nabla u}), (\tilde{\boldsymbol{v}}_a + \boldsymbol{\delta}_a) \big\rangle + \big\langle \partial_d \Delta\mathbb{J}(\boldsymbol{u}, \boldsymbol{\nabla u}), \boldsymbol{\nabla \delta}_a \big\rangle \leq a^{3/2} (\|\tilde{\boldsymbol{v}}_a\|_{L^2(\Omega)} + \|\boldsymbol{\delta}_a\|_{H^1(\Omega)}) \\ \leq Ca^4, \tag{37d}$$

the last inequality stemming from estimates (20).

The term $\langle \partial_d \Delta \mathbb{J}(\boldsymbol{u}, \boldsymbol{\nabla u}), \boldsymbol{\nabla} \tilde{\boldsymbol{v}}_a \rangle$ remains to be estimated. By the mean value theorem applied to $\partial_d(\Delta\psi)(\boldsymbol{x}, \boldsymbol{u}(\boldsymbol{x}), \boldsymbol{\nabla u}(\boldsymbol{x}))$, there exists $t(\boldsymbol{x}) \in [0,1]$ such that

$$\begin{aligned}\partial_d(\Delta\psi)(\boldsymbol{x}, \boldsymbol{u}(\boldsymbol{x}), \boldsymbol{\nabla u}(\boldsymbol{x})) = \partial_d(\Delta\psi)(\boldsymbol{z}, \boldsymbol{u}(\boldsymbol{z}), \boldsymbol{\nabla u}(\boldsymbol{z})) + \partial^2_{xd}\Delta\psi(\boldsymbol{x}_t, \boldsymbol{u}_t, \boldsymbol{\nabla u}_t)\cdot(\boldsymbol{x}-\boldsymbol{z}) \\ + \partial^2_{ud}\Delta\psi(\boldsymbol{x}_t, \boldsymbol{u}_t, \boldsymbol{\nabla u}_t)\cdot[\boldsymbol{u}(\boldsymbol{x})-\boldsymbol{u}(\boldsymbol{z})] + \partial^2_{dd}\Delta\psi(\boldsymbol{x}_t, \boldsymbol{u}_t, \boldsymbol{\nabla u}_t) : [\boldsymbol{\nabla u}(\boldsymbol{x})-\boldsymbol{\nabla u}(\boldsymbol{z})]\end{aligned}$$

where $\boldsymbol{x}_t$, $\boldsymbol{u}_t$, $\boldsymbol{\nabla u}_t$ are defined by

$$\begin{aligned}\boldsymbol{x}_t &:= \boldsymbol{z} + t(\boldsymbol{x}-\boldsymbol{z}), \\ \boldsymbol{u}_t &:= \boldsymbol{u}(\boldsymbol{z}) + t[\boldsymbol{u}(\boldsymbol{x})-\boldsymbol{u}(\boldsymbol{z})], \\ \boldsymbol{\nabla u}_t &:= \boldsymbol{\nabla u}(\boldsymbol{z}) + t[\boldsymbol{\nabla u}(\boldsymbol{x})-\boldsymbol{\nabla u}(\boldsymbol{z})].\end{aligned} \tag{37e}$$

Introducing $\boldsymbol{x}-\boldsymbol{z} = a\bar{\boldsymbol{x}}$ and expansions (34i), stemming from the C^2 interior regularity of $\boldsymbol{u}$, in the above definitions, one obtains for $\boldsymbol{x} \in B_a$

$$\partial_d(\Delta\psi)(\boldsymbol{x}, \boldsymbol{u}(\boldsymbol{x}), \boldsymbol{\nabla u}(\boldsymbol{x})) = \partial_d(\Delta\psi)(\boldsymbol{z}, \boldsymbol{u}(\boldsymbol{z}), \boldsymbol{\nabla u}(\boldsymbol{z})) + O(a)$$

which in turn implies

$$\langle \partial_d \Delta \mathbb{J}(\boldsymbol{u}, \boldsymbol{\nabla u}), \boldsymbol{\nabla} \tilde{\boldsymbol{v}}_a \rangle = a^3 \partial_d(\Delta\psi)(\boldsymbol{z}, \boldsymbol{u}(\boldsymbol{z}), \boldsymbol{\nabla u}(\boldsymbol{z})) : \int_{\mathcal{B}} \boldsymbol{\nabla v}_{\mathcal{B}} \, \mathrm{d}V + o(a^3) \tag{37f}$$

The lemma finally follows by substituting (37d) and (37f) into the right-hand side of (37c) and then using the resulting estimate together with (37b) in (37a). □

The two-dimensional case. The proof for the two-dimensional plane-strain case is identical, except for the fact that estimates (20) to (22) must be replaced by their following two-dimensional counterparts:

$$\text{(a)} \ \ \|\boldsymbol{\nabla}\tilde{\boldsymbol{v}}_a\|_{L^2(\Omega;\mathbb{R}^2)} \le Ca, \qquad \text{(b)} \ \ \|\tilde{\boldsymbol{v}}_a\|_{L^2(\Omega;\mathbb{R}^2)} \le Ca^2\sqrt{|\log a|}, \qquad \text{(c)} \ \ \|\boldsymbol{\delta}_a\|_{H^1(\Omega;\mathbb{R}^2)} \le Ca^2, \tag{38a}$$

$$\text{(a)} \ \ \|\boldsymbol{\nabla v}_a\|_{L^2(\Omega;\mathbb{R}^2)} \le Ca, \qquad \text{(b)} \ \ \|\boldsymbol{v}_a\|_{L^2(\Omega;\mathbb{R}^2)} \le Ca^2. \tag{38b}$$

$$\|\boldsymbol{\nabla}\tilde{\boldsymbol{v}}_a\|_{L^\infty(\Omega\setminus D)} \le Ca^2, \tag{38c}$$

which can be established e.g. by adapting to the two-dimensional case the proofs given in [15].

3.2 Case of piecewise-regular cost functional densities

Now we extend the previous results to the topological derivative of functionals J_ω defined by an integral over a portion $\omega \subset \Omega$ of the elastic body Ω, of the form

$$J_\omega(\boldsymbol{\mathcal{C}}_a) = \mathbb{J}_a(\boldsymbol{u}_a, \boldsymbol{\nabla u}_a; \omega), \qquad \text{with} \ \ \mathbb{J}_a(\boldsymbol{u}, \boldsymbol{d}; \omega) = \int_\omega \psi_a(\boldsymbol{x}, \boldsymbol{u}, \boldsymbol{\nabla u}) \, \mathrm{d}V(\boldsymbol{x}),$$

where the trial inhomogeneity B_a is assumed to satisfy either $B_a \Subset \omega$ or $B_a \Subset (\Omega \setminus \bar{\omega})$ (the case where $\overline{B_a} \cap \partial\omega \neq \emptyset$ not being considered). If $B_a \Subset \omega$, the previous analysis remains valid, with $\mathrm{D}J$ still given by (28) and the only change concerning the adjoint solution, which now satisfies the weak formulation

$$\int_\Omega \boldsymbol{\varepsilon}[\boldsymbol{p}] : \boldsymbol{\mathcal{C}} : \boldsymbol{\varepsilon}[\boldsymbol{q}] dV = \int_\Omega \chi_\omega \big\{ \partial_d\psi : \boldsymbol{\nabla q} + \partial_u\psi \cdot \boldsymbol{q} \big\} \, \mathrm{d}V, \qquad \forall \boldsymbol{q} \in W_0(\Omega). \tag{39}$$

On the other hand, if $B_a \Subset (\Omega \setminus \bar{\omega})$, $\psi_a - \psi = 0$ in ω and the cut-off function θ in decomposition (19) can be chosen, for any sufficiently small a, such that $\theta = 0$ in ω. This choice implies

that $\boldsymbol{v}_a = \boldsymbol{\delta}_a$ in ω for any $\boldsymbol{z} \in \Omega \backslash \overline{\omega}$, and hence, by estimate (20c), that

$$\|\boldsymbol{v}_a\|_{H^1(\omega)} \leq C a^{5/2}.$$

Consequently, retracing the proof of Theorem 1, contributions to $\mathrm{D}J$ arising from $\partial_{dd}\psi$ and $\partial_{dd}\psi^\star$ in Lemma 4 are $o(a^3)$, and $\mathrm{D}J$ is simply given, in terms of the solutions $\boldsymbol{u}$ of (3) and $\boldsymbol{p}$ of (39), by

$$\mathrm{D}J(\boldsymbol{z}) = -\boldsymbol{\nabla}\boldsymbol{p}(\boldsymbol{z}) : \boldsymbol{\mathcal{A}} : \boldsymbol{\nabla}\boldsymbol{u}(\boldsymbol{z}). \tag{40}$$

Regularity of the adjoint solution. As it was previously seen, the point-wise evaluation of $\mathrm{D}J$ at some $\boldsymbol{z} \in \Omega$ requires the background displacement $\boldsymbol{u}$ and the adjoint solution $\boldsymbol{p}$ to have some local regularity at $\boldsymbol{z}$, namely $\boldsymbol{u}, \boldsymbol{p} \in C^{2,\alpha}(D;\mathbb{R}^3)$ for some neighborhood $D \Subset \Omega$ of $\boldsymbol{z}$ and $\alpha \in (0,1)$. The needed regularity for $\boldsymbol{u}$ follows directly from the regularity of the body force density $\boldsymbol{f} \in C^{0,\alpha}(\Omega;\mathbb{R}^3)$. When the cost function J depends only on $\boldsymbol{u}$, the adjoint state $\boldsymbol{p}$ solves

$$\text{Find} \;\; \boldsymbol{p} \in W_0, \qquad \langle \boldsymbol{p}, \boldsymbol{w} \rangle_\Omega^{\mathcal{C}} = \big\langle \partial_u \mathbb{J}_0(\boldsymbol{u}), \boldsymbol{w} \big\rangle, \quad \forall \boldsymbol{w} \in W_0.$$

Then, if $\partial_u \psi(\boldsymbol{x}, \boldsymbol{u}(\boldsymbol{x})) \in C^{0,\alpha}(\Omega;\mathbb{R}^3)$, $\boldsymbol{p}$ fulfills automatically the required interior regularity in Ω. On the contrary, the case when the cost functional depends on $\boldsymbol{\nabla}\boldsymbol{u}$ is slightly more delicate. In such a case $\boldsymbol{p}$ solves

$$\text{Find} \;\; \boldsymbol{p} \in W_0, \qquad \langle \boldsymbol{p}, \boldsymbol{w} \rangle_\Omega^{\mathcal{C}} = \big\langle \partial_d \mathbb{J}_0(\boldsymbol{\nabla}\boldsymbol{u}), \boldsymbol{\nabla}\boldsymbol{w} \big\rangle, \quad \forall \boldsymbol{w} \in W_0$$

Thus if $\partial_d \psi(\boldsymbol{x}, \boldsymbol{\nabla}\boldsymbol{u}(\boldsymbol{x})) \in C^{1,\alpha}(\Omega;\mathbb{R}^{3\times 3})$, $\boldsymbol{p}$ fulfills the required regularity. We remark that the components of the tensor $(\boldsymbol{\nabla} u)_{ij} \in C^{1,\alpha}(\Omega)$ so we can take any function $\psi(\cdot, d) \in C^1(\mathbb{R}^{3\times 3})$ for this purpose. Finally when the cost function $\mathbb{J}$ is defined in a sub-domain ω of Ω,

$$\big\langle \partial_d \mathbb{J}_0(\boldsymbol{\nabla}\boldsymbol{u}), \boldsymbol{\nabla}\boldsymbol{w} \big\rangle = \int_\omega \partial_d \psi(\boldsymbol{x}, \boldsymbol{\nabla}\boldsymbol{u}) : \boldsymbol{\nabla}\boldsymbol{w} \, \mathrm{d}V = \int_\Omega \chi_\omega \partial_d \psi(\boldsymbol{x}, \boldsymbol{\nabla}\boldsymbol{u}(\boldsymbol{x})) : \boldsymbol{\nabla}\boldsymbol{w} \, \mathrm{d}V,$$

the adjoint state $\boldsymbol{p}$ solves

$$\begin{cases} -\mathrm{div}(\boldsymbol{\mathcal{C}}\boldsymbol{\varepsilon}(\boldsymbol{p})) = -\mathrm{div}(\partial_d \psi(\boldsymbol{x}, \boldsymbol{\nabla}\boldsymbol{u})) & \text{in } D, \\ \boldsymbol{p} = \boldsymbol{0} & \text{on } \Gamma_D, \\ \boldsymbol{\mathcal{C}} : \boldsymbol{\varepsilon}(\boldsymbol{p}) \cdot \boldsymbol{n} = \boldsymbol{0} & \text{on } \Gamma_N, \end{cases}$$

where $\Gamma_N \cap \omega = \emptyset$ is assumed. We can easily check that $\mathrm{div}(\chi_\omega \partial_d \psi(\boldsymbol{x}, \boldsymbol{\nabla}\boldsymbol{u}(\boldsymbol{x}))) \in H^{-1}(\Omega;\mathbb{R}^3)$ if $\partial_d \psi(\boldsymbol{x}, \boldsymbol{\nabla}\boldsymbol{u}(\boldsymbol{x})) \in C^{1,\alpha}(\Omega;\mathbb{R}^{3\times 3})$. Then by the Lax-Milgram theorem $\boldsymbol{p} \in W_0(\Omega)$. To achieve the required $C^{2,\alpha}$ local regularity of $\boldsymbol{p}$ at $\boldsymbol{z} \in \Omega$, we only need to select $\boldsymbol{z} \notin \partial\omega$.

Indeed, if $\boldsymbol{z} \in (\Omega \setminus \bar{\omega})$, there is a smooth neighborhood $D \subset \Omega \setminus \bar{\omega}$ of $\boldsymbol{z}$ such that $\mathrm{div}(\boldsymbol{\mathcal{C}} : \boldsymbol{\varepsilon}(\boldsymbol{p})) = 0$ in D. Therefore (e.g. [35, Theorem 4.16]), there exists a neighborhood $D' \Subset D$ of $\boldsymbol{z}$ where $\boldsymbol{p} \in C^{2,\alpha}(D';\mathbb{R}^3)$.

Otherwise if $\boldsymbol{z} \in \omega$, there exists a smooth neighborhood $D \Subset \omega$ of $\boldsymbol{z}$ where $\boldsymbol{p}$ solves the problem

$$\begin{cases} -\mathrm{div}(\boldsymbol{\mathcal{C}}\boldsymbol{\varepsilon}(\boldsymbol{q})) = -\mathrm{div}(\partial_d \psi(\boldsymbol{x}, \boldsymbol{\nabla}\boldsymbol{u})) & \text{in } D, \\ \boldsymbol{q} = \boldsymbol{p} & \text{on } \partial D. \end{cases}$$

The adjoint state $\boldsymbol{p}$ can be decomposed as $\boldsymbol{p} = \boldsymbol{p}_1 + \boldsymbol{p}_2$, where $\boldsymbol{p}_1$ solves the problem

$$\begin{cases} -\mathrm{div}(\boldsymbol{\mathcal{C}}\boldsymbol{\varepsilon}(\boldsymbol{q})) = \boldsymbol{0} & \text{in } D, \\ \boldsymbol{q} = \boldsymbol{p} & \text{on } \partial D \end{cases}$$

and $\boldsymbol{p}_2$ solves

$$\begin{cases} -\mathrm{div}(\boldsymbol{\mathcal{C}}\boldsymbol{\varepsilon}(\boldsymbol{q})) = -\mathrm{div}(\partial_d\psi(\boldsymbol{x},\boldsymbol{\nabla u})) & \text{in } D, \\ \boldsymbol{q} = \boldsymbol{0} & \text{on } \partial D. \end{cases}$$

Therefore, there exists a neighborhood $D' \Subset D$ of $\boldsymbol{z}$ where $\boldsymbol{p}_1 \in C^{2,\alpha}(D';\mathbb{R}^3)$. Moreover $\boldsymbol{p}_2 \in C^{2,\alpha}(D;\mathbb{R}^3)$ if $\partial_d\psi(\boldsymbol{x},\boldsymbol{\nabla u}(\boldsymbol{x})) \in C^{1,\alpha}(D;\mathbb{R}^{3\times 3})$, thanks to the interior regularity of $\boldsymbol{p}_2$. Hence $\boldsymbol{p} \in C^{2,\alpha}(D';\mathbb{R}^3)$.

3.3 Particular cases

A few particular instances of the general result given by Theorem 1, and their connections to previously-available results, are now discussed.

Displacement-based functional. In this case, $\partial_d\psi = \partial_d\psi^\star = 0$, and hence $\mathcal{G} = \mathcal{G}^\star = 0$. Only the first two terms in the expression (28) of $\mathrm{D}J$ then remain; moreover the second term in the right-hand side of the adjoint problem (35) vanishes. As a result, formula (28) reduces to known results for displacement-based functionals, e.g. [15, Prop. 4.2] if $\Delta\psi(\boldsymbol{z},\boldsymbol{u}(\boldsymbol{z})) = 0$.

Quadratic stress-based functional. This case is such that $\partial^2_{dd}\psi = \boldsymbol{\mathcal{D}}(\boldsymbol{z})$, $\partial^2_{dd}\psi^\star = \boldsymbol{\mathcal{D}}^\star(\boldsymbol{z})$, where $\boldsymbol{\mathcal{D}}$ and $\boldsymbol{\mathcal{D}}^\star$ are symmetric fourth-order tensor fields. It is studied in [40], where $\boldsymbol{\mathcal{D}}$ and $\boldsymbol{\mathcal{D}}^\star$ are constant, and otherwise arbitrary, tensors. Expression (28) of $\mathrm{D}J$ for this case is indeed found, after adjusting for notational differences, to coincide with [40, Theorem 3.1]. Reference [40] also gives a number of useful explicit formulas on Eshelby's solution and its use in evaluating $\mathrm{D}J$ for quadratic stress-based functional, including one for the evaluation of the last two integrals in (28) when $\mathcal{B}$ is the unit sphere and the tensor $\boldsymbol{\mathcal{D}}$ is isotropic.

Quadratic energy-like functional. This case, examined in [15], is a particular instance of the previous case with $\boldsymbol{\mathcal{D}} = \boldsymbol{\mathcal{C}}$ and $\boldsymbol{\mathcal{D}}^\star = \boldsymbol{\mathcal{C}}^\star$, and thus corresponds to functionals of the form

$$\mathbb{J}_a(\boldsymbol{\nabla u}) = \big\langle \boldsymbol{u}-\boldsymbol{u}_0, \boldsymbol{u}-\boldsymbol{u}_0 \big\rangle_\Omega^{\mathcal{C}_a} \quad (\boldsymbol{u}_0 \in H^1(\Omega;\mathbb{R}^3) \text{ given}).$$

Apply our main result (28) to this case yields

$$\begin{aligned} \mathrm{D}J(\boldsymbol{z}) &= |\mathcal{B}|\boldsymbol{\varepsilon}[\boldsymbol{u}-\boldsymbol{u}_0](\boldsymbol{z}) : \Delta\boldsymbol{\mathcal{C}} : \boldsymbol{\varepsilon}[\boldsymbol{u}-\boldsymbol{u}_0](\boldsymbol{z}) - \boldsymbol{\varepsilon}[\boldsymbol{p}](\boldsymbol{z}) : \boldsymbol{\mathcal{A}} : \boldsymbol{\varepsilon}[\boldsymbol{u}](\boldsymbol{z}) \\ &\quad + |\mathcal{B}|\boldsymbol{\varepsilon}[\boldsymbol{u}-2\boldsymbol{u}_0](\boldsymbol{z}) : \Delta\boldsymbol{\mathcal{C}} : \int_{\mathcal{B}} \boldsymbol{\varepsilon}[\boldsymbol{v}_{\mathcal{B}}]\,\mathrm{d}V \\ &= |\mathcal{B}|\boldsymbol{\varepsilon}[\boldsymbol{u}_0](\boldsymbol{z}) : \Delta\boldsymbol{\mathcal{C}} : \boldsymbol{\varepsilon}[\boldsymbol{u}_0](\boldsymbol{z}) + \boldsymbol{\varepsilon}[\boldsymbol{u}-2\boldsymbol{u}_0-\boldsymbol{p}](\boldsymbol{z}) : \boldsymbol{\mathcal{A}} : \boldsymbol{\varepsilon}[\boldsymbol{u}](\boldsymbol{z}) \end{aligned} \tag{41}$$

where the last expression matches the one established by another approach in [15] (wherein the adjoint solution $\boldsymbol{q}$ is linked to $\boldsymbol{p}$ through $\boldsymbol{q} = \boldsymbol{u}_0 - \boldsymbol{u} + \boldsymbol{p}$). We have used identities

$$\int_{\mathbb{R}^3} \boldsymbol{\varepsilon}[\boldsymbol{v}_{\mathcal{B}}] : \boldsymbol{\mathcal{C}}_a : \boldsymbol{\varepsilon}[\boldsymbol{v}_{\mathcal{B}}]\,\mathrm{d}V = -|\mathcal{B}|\boldsymbol{\varepsilon}[\boldsymbol{u}](\boldsymbol{z}) : \Delta\boldsymbol{\mathcal{C}} : \int_{\mathcal{B}} \boldsymbol{\varepsilon}[\boldsymbol{v}_{\mathcal{B}}]\,\mathrm{d}V$$

(obtained from (11) with $\boldsymbol{w} = \boldsymbol{v}_{\mathcal{B}}$) in the first equality of (41), and

$$|\mathcal{B}|\boldsymbol{\varepsilon}[\boldsymbol{u}-2\boldsymbol{u}_0] : \Delta\boldsymbol{\mathcal{C}} : \int_{\mathcal{B}} \boldsymbol{\varepsilon}[\boldsymbol{v}_{\mathcal{B}}]\,\mathrm{d}V = \boldsymbol{\varepsilon}[\boldsymbol{u}-2\boldsymbol{u}_0] : \big(\boldsymbol{\mathcal{A}} - |\mathcal{B}|\Delta\boldsymbol{\mathcal{C}}\big) : \boldsymbol{\varepsilon}[\boldsymbol{u}](\boldsymbol{z})$$

(resulting from left multiplication of (15) by $\boldsymbol{\varepsilon}[\boldsymbol{u}-2\boldsymbol{u}_0]$) in the second equality of (41).

Drucker-Prager penalty functional. The penalty functional considered in [7] is based on the following assumptions: (a) two-dimensional isotropic elasticity, plane-strain conditions, identical Poisson ratio in background and inhomogeneity materials, (b) circular trial inhomogeneities (i.e. $\mathcal{B}$ taken as the unit disk), (c) $\psi(\boldsymbol{d}) = \Psi_n(\alpha^2_{\mathrm{DP}}(\boldsymbol{\mathcal{C}} : \boldsymbol{d}))$, with α^2_{DP} denoting the yield function associated with the Drucker-Prager criterion, and a similar definition for $\psi^\star$ in terms of the inhomogeneity material. Using these assumptions in equation (28), we recover equation (44) of [7] as a special case.

4 Numerical evaluation of the topological derivative

The evaluation of the topological derivative (28) requires numerical procedures, even in the simplest cases (isotropic elasticity, spherical shape for $\mathcal{B}$), in particular because of the integral over the unbounded region $\mathbb{R}^3 \backslash \mathcal{B}$. The details of such procedure depend upon whether $\mathcal{B}$ is an ellipsoid, or has some other shape, as $\boldsymbol{\nabla} \boldsymbol{v}_{\mathcal{B}}$ is constant inside $\mathcal{B}$ in the former case but not necessarily in the latter [18]. In the sequel, we concentrate on the ellipsoidal case, which is sufficient for most applications.

4.1 3D case, ellipsoidal trial inclusion

Let $\mathcal{B}$ denote an ellipsoid with principal axes a_1, a_2, a_3, as in Section 2.2. In that case, $\boldsymbol{\nabla} \boldsymbol{v}_{\mathcal{B}}(\bar{\boldsymbol{x}})$ inside $\mathcal{B}$ is given by (12), and the two integrals over $\mathcal{B}$ appearing in (28) are easily evaluated since their densities are constant.

The integral over $\mathbb{R}^3 \setminus \mathcal{B}$ in (28) requires a more elaborate procedure, as the integration domain is unbounded and $\boldsymbol{v}_{\mathcal{B}}$ is spatially-dependent (and in fact decays at infinity). First $\bar{\boldsymbol{x}}$ is transformed to $\boldsymbol{y}$ according to

$$\boldsymbol{y} = (\bar{x}_1/a_1, \bar{x}_2/a_2, \bar{x}_3/a_3) \qquad (|\boldsymbol{y}| \geq 1). \tag{42}$$

It is then natural to set $\boldsymbol{y} = |\boldsymbol{y}|\hat{\boldsymbol{y}}$, with $\hat{\boldsymbol{y}} \in S^2$ (where S^2 is the unit sphere) and $1 \leq |\boldsymbol{y}| \leq +\infty$. Finally the transformation $t = |\boldsymbol{y}|^{-1}$ (with $0 < t \leq 1$) is applied to the radial variable, so that (42) represents any $\bar{\boldsymbol{x}} \in \mathbb{R}^3 \setminus \mathcal{B}$ in the form $\bar{\boldsymbol{x}}(\hat{\boldsymbol{y}}, t)$. This results in

$$\int_{\mathbb{R}^3 \setminus \mathcal{B}} \mathcal{G}(\boldsymbol{z}, \boldsymbol{\nabla} \boldsymbol{v}_{\mathcal{B}}(\bar{\boldsymbol{x}}))\, \mathrm{d}V(\bar{\boldsymbol{x}}) = \frac{1}{a_1 a_2 a_3} \int_0^1 \frac{1}{t^4} \Big\{ \int_{S^2} \mathcal{G}(\boldsymbol{z}, \boldsymbol{\nabla} \boldsymbol{v}_{\mathcal{B}}(\bar{\boldsymbol{x}}(\hat{\boldsymbol{y}}, t)))\, \mathrm{d}S(\hat{\boldsymbol{y}}) \Big\}\, \mathrm{d}t, \tag{43}$$

which is to be evaluated using numerical quadrature (using e.g. a Gaussian rule for t and a Lebedev rule on S^2 [32]).

The exterior Eshelby tensor and its numerical evaluation. Equation (43) in turn requires the evaluation of $\boldsymbol{\nabla} \boldsymbol{v}_{\mathcal{B}}(\bar{\boldsymbol{x}}(\hat{\boldsymbol{y}}, t))$ for any given quadrature point $(\hat{\boldsymbol{y}}, t)$. Having assumed an ellipsoidal shape for $\mathcal{B}$, $\boldsymbol{\nabla} \boldsymbol{v}_{\mathcal{B}}$ is given outside of $\mathcal{B}$ by (Eq. (18.6) of [37])

$$\boldsymbol{\nabla} \boldsymbol{v}_{\mathcal{B}}(\bar{\boldsymbol{x}}) = \boldsymbol{\mathcal{S}}^{\mathrm{ext}}(\bar{\boldsymbol{x}}) : \boldsymbol{\varepsilon}^\star, \tag{44}$$

where $\boldsymbol{\varepsilon}^\star$ is again defined by (12) and $\boldsymbol{\mathcal{S}}^{\mathrm{ext}}(\bar{\boldsymbol{x}})$ is the exterior (spatially varying) Eshelby tensor, given by

$$\mathcal{S}^{\mathrm{ext}}_{ijmn}(\bar{\boldsymbol{x}}(\hat{\boldsymbol{y}}, t)) = \frac{1}{2\pi} \mathcal{C}_{k\ell mn} \Big\{ \int_{S^\star(\hat{\boldsymbol{y}}, t)} N_{ik}(\boldsymbol{\xi}) \xi_\ell \xi_j\, \mathrm{d}S(\hat{\boldsymbol{s}}) - \oint_{L^+(\hat{\boldsymbol{y}}, t)} t N_{ik}(\boldsymbol{\xi}) \xi_\ell \xi_j\, \mathrm{d}\phi(\hat{\boldsymbol{s}}) \Big\}, \tag{45}$$

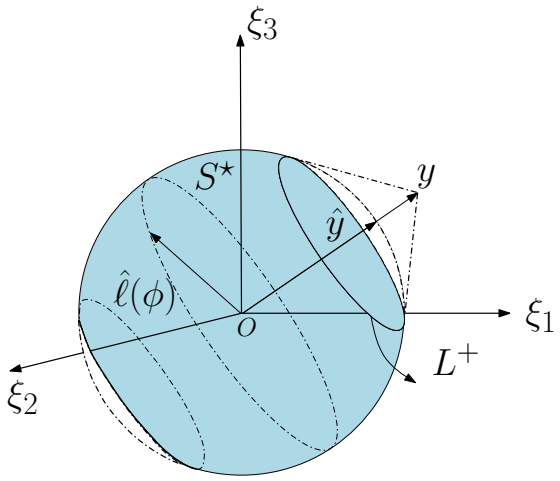

Figure 1: Parametrization of the set $S^\star \subset S^2$.

where $\boldsymbol{\xi} = \boldsymbol{\xi}(\hat{\boldsymbol{s}})$ and $\boldsymbol{N}(\boldsymbol{\xi})$ are defined as in (13), $S^\star(\hat{\boldsymbol{y}}, t)$ is the portion of S^2 defined by $S^\star(\hat{\boldsymbol{y}}, t) := \{\hat{\boldsymbol{s}} \in S^2 : 0 \leq \hat{\boldsymbol{s}} \cdot \hat{\boldsymbol{y}} \leq t\}$, $L^+(\hat{\boldsymbol{y}}, t)$ the circular contour on S^2 defined by $L^+(\hat{\boldsymbol{y}}, t) := \{\hat{\boldsymbol{s}} \in S^2 : \hat{\boldsymbol{s}} \cdot \hat{\boldsymbol{y}} = t\}$ (Fig. 1), while $\mathrm{d}S(\hat{\boldsymbol{s}})$ and $\mathrm{d}\phi(\hat{\boldsymbol{s}})$ respectively denote the solid angle differential on S^2 and the polar angle differential on the circle $L^+(\hat{\boldsymbol{y}}, t)$. We note that definition (44) of $\boldsymbol{\mathcal{S}}^{\mathrm{ext}}(\bar{\boldsymbol{x}})$ again differs somewhat from the symmetrized version used in e.g. [40].

It is useful to recast (45) in a form more suitable for numerical quadrature. To this end, let $S^\star(\hat{\boldsymbol{y}}, t)$ be represented in terms of coordinates (z, ϕ) spanning the fixed domain $Q := \big\{(z, \phi) \in [0, 1] \times [0, 2\pi[\big\}$ by

$$S^\star(\hat{\boldsymbol{y}}, t) = \left\{ \; \hat{\boldsymbol{s}} \in S^2 \;\middle|\; \hat{\boldsymbol{s}} = (1 - t^2 z^2)^{1/2} \hat{\boldsymbol{\ell}}(\phi) + tz\hat{\boldsymbol{y}} \; \right\}$$

with $\hat{\boldsymbol{\ell}}(\phi)$ spanning the unit circle $S^1 := \{\hat{\boldsymbol{s}} \cdot \hat{\boldsymbol{y}} = 0\}$ (this representation stems from parameterizing $\hat{\boldsymbol{s}}$ using angular spherical coordinates (θ, ϕ) and setting $z := t^{-1} \cos\theta$). $L^+(\hat{\boldsymbol{y}}, t)$ is then the subset of $S^\star(\hat{\boldsymbol{y}}, t)$ such that $z = 1$. The (z, ϕ) parametrization implies that $\mathrm{d}S(\hat{\boldsymbol{s}}) = t \, \mathrm{d}z \, \mathrm{d}\phi$, and also induces a corresponding representation $\boldsymbol{\xi}(tz, \phi)$ of $\boldsymbol{\xi}$ as defined by (14). Inserting it in (45) and rearranging the resulting expression, the exterior Eshelby tensor $\boldsymbol{\mathcal{S}}^{\mathrm{ext}}$ is given, for a given evaluation point $\bar{\boldsymbol{x}}(\hat{\boldsymbol{y}}, t)$, by an integral over the fixed domain Q:

$$\mathcal{S}^{\mathrm{ext}}_{ijmn}(\bar{\boldsymbol{x}}(\hat{\boldsymbol{y}}, t)) = \frac{t}{2\pi} \mathcal{C}_{k\ell mn} \int_0^1 \mathrm{d}z \int_0^{2\pi} \big[\Sigma_{k\ell ij}(tz, \phi) - \Sigma_{k\ell ij}(t, \phi)\big] \, \mathrm{d}\phi \tag{46}$$

with

$$\Sigma_{k\ell ij}(tz, \phi) = N_{ik}(\boldsymbol{\xi}(tz, \phi)) \xi_\ell(tz, \phi) \xi_j(tz, \phi).$$

For given $\bar{\boldsymbol{x}}(\hat{\boldsymbol{y}}, t)$, $\boldsymbol{\mathcal{S}}^{\mathrm{ext}}(\bar{\boldsymbol{x}}(\hat{\boldsymbol{y}}, t))$ can then be evaluated by means of standard numerical quadrature in Q (using e.g. product rules that are Gaussian in z and uniform in ϕ). In addition, a Taylor expansion in t about $t = 0$ yields $\Sigma_{k\ell ij}(tz, \phi) - \Sigma_{k\ell ij}(t, \phi) = (z - 1)\partial_1 \Sigma_{k\ell ij}(0, \phi) + O(t^2)$, where ∂_1 denotes the partial derivative w.r.t. the first argument. It is moreover straightforward to show that $\partial_1 \Sigma_{k\ell ij}(0, \phi)$ is for any $(k\ell ij)$ a polynomial in $(\cos\phi, \sin\phi)$ involving only odd-degree terms, and hence that its integral over $\phi \in [0, 2\pi]$ vanishes. Consequently, the Taylor expansion of (46) about $t = 0$ is $\mathcal{S}^{\mathrm{ext}}_{ijmn}(\bar{\boldsymbol{x}}(\hat{\boldsymbol{y}}, t)) = O(t^3)$, implying that the integral in t of (43) is well defined. This remark is consistent with the otherwise known $O(|\bar{\boldsymbol{x}}|^{-3})$ behavior of $\boldsymbol{\nabla} \boldsymbol{v}_{\mathcal{B}}(\bar{\boldsymbol{x}})$ as $|\bar{\boldsymbol{x}}| \to +\infty$.

Remark 5. *For a general functional with non-quadratic dependence on stress (i.e. such that $\partial_d^2 d\psi$ and $\partial_d^2 d\psi^\star$ depend on $\boldsymbol{d}$), the computation of* (43) *by numerical quadrature must be done anew for each evaluation point $\boldsymbol{z}$ of $DJ(\boldsymbol{z})$. This makes the computation of the topological derivative* field *DJ potentially expensive.*

On the other hand, quadratic stress-based functionals entail much less computational work, since one has (with $\boldsymbol{\mathcal{D}}$ as in Theorem 1)

$$\int_{\mathbb{R}^3\setminus\mathcal{B}} \mathcal{G}(\boldsymbol{z},\boldsymbol{\nabla v}_{\mathcal{B}}(\bar{\boldsymbol{x}}))\; dV(\bar{\boldsymbol{x}}) = \boldsymbol{\varepsilon}^\star(\boldsymbol{z}) : \Big\{ \frac{1}{2}\int_{\mathbb{R}^3\setminus\mathcal{B}} \boldsymbol{\mathcal{S}}^{ext}(\bar{\boldsymbol{x}}) : \boldsymbol{\mathcal{D}}(\boldsymbol{z}) : \boldsymbol{\mathcal{S}}^{ext}(\bar{\boldsymbol{x}})\; dV(\bar{\boldsymbol{x}}) \Big\} : \boldsymbol{\varepsilon}^\star(\boldsymbol{z}),$$

allowing the computation of the whole field $DJ(\boldsymbol{z})$ using just one numerical quadrature in the $(\hat{\boldsymbol{y}},t)$ variables (if $\boldsymbol{\mathcal{D}}$ is independent of $\boldsymbol{z}$) or up to 45 such quadratures (for general $\boldsymbol{\mathcal{D}}(\boldsymbol{z})$, for which the major symmetry $\mathcal{D}_{ijk\ell} = \mathcal{D}_{k\ell ij}$ necessarily holds).

Isotropic background material. Letting the material be in that case characterized using its shear modulus G and Poisson's ratio ν, the Christoffel tensor $\boldsymbol{N}$ has a simple closed-form expression

$$N_{ik}(\boldsymbol{\xi}) = \frac{1}{G|\boldsymbol{\xi}|^2}\Big[\delta_{ik} - \frac{1}{2(1-\nu)}\hat{\xi}_i \otimes \hat{\xi}_k\Big] \tag{47}$$

with $\hat{\boldsymbol{\xi}} := \boldsymbol{\xi}/|\boldsymbol{\xi}|$. A straightforward calculation then shows that $\mathcal{C}_{k\ell mn}\Sigma_{k\ell ij} = \mathcal{C}_{k\ell mn}\Sigma_{k\ell ji}$, implying that $\boldsymbol{\mathcal{S}}^{\rm ext}(\bar{\boldsymbol{x}}) : \boldsymbol{\varepsilon}^\star$ is symmetric, i.e. coincides with the value obtained from the definition of the exterior Eshelby tensor used in [40]. The exterior Eshelby tensor for a unit ball is then found (by analytical evaluation of (46) using (47), or by completing derivations presented in [37, Sec. 11]) to have the following closed-form expression (wherein $\bar{x} := |\bar{\boldsymbol{x}}|$):

$$\begin{aligned} 2(1-\nu)\mathcal{S}^{\rm ext}_{ijk\ell}(\bar{\boldsymbol{x}}) = {} & \Big[\frac{7}{\bar{x}^9} - \frac{5}{\bar{x}^7}\Big] x_i x_j x_k x_\ell + \Big[\frac{1}{\bar{x}^5} - \frac{1}{\bar{x}^7}\Big]\delta_{ij}x_k x_\ell + \Big[\frac{1-2\nu}{\bar{x}^5} - \frac{1}{\bar{x}^7}\Big]\delta_{k\ell}x_i x_j \\ & + \Big[\frac{\nu}{\bar{x}^5} - \frac{1}{\bar{x}^7}\Big](\delta_{ik}x_j x_\ell + \delta_{jk}x_i x_\ell + \delta_{i\ell}x_j x_k + \delta_{j\ell}x_i x_k) \\ & + \Big[\frac{1}{5\bar{x}^5} - \frac{1-2\nu}{3\bar{x}^3}\Big]\delta_{ij}\delta_{k\ell} + \Big[\frac{1}{5\bar{x}^5} + \frac{1-2\nu}{3\bar{x}^3}\Big](\delta_{ik}\delta_{j\ell} + \delta_{jk}\delta_{i\ell}). \end{aligned} \tag{48}$$

Moreover, $\boldsymbol{\mathcal{S}}^{\rm ext}(\bar{\boldsymbol{x}}) : \boldsymbol{E}$ evaluated for an arbitrary tensor $\boldsymbol{E} \in \mathbb{R}^{3\times3}_{\rm sym}$ using the above formula coincides with equation (23) of [40].

4.2 2D plane strain case, elliptical trial inclusion.

The exterior Eshelby tensor for an elliptic inclusion

$$\mathcal{B} = \big\{\boldsymbol{x} \in \mathbb{R}^2,\ (x_1/a_1)^2 + (x_2/a_2)^2 \le 1\big\}, \quad a_1, a_2 > 0,$$

embedded in a 2D infinite anisotropic medium, under plane strain conditions, can also be expressed (following a direct derivation given in Appendix A) as an integral in a form suitable for numerical quadrature.

$$\begin{aligned} \boldsymbol{\mathcal{S}}^{\rm ext}(\bar{\boldsymbol{x}}) = {} & \frac{1}{\pi}\Big\{\int_{-\pi/2}^{\pi/2} \Big[\,\boldsymbol{\alpha}(\theta)\otimes\boldsymbol{N}\big(\boldsymbol{\alpha}(\theta)\big)\otimes\boldsymbol{\alpha}(\theta)\,\Big]\ \mathrm{d}\theta\Big\} : \boldsymbol{\mathcal{C}} \\ & - \frac{2}{\pi}\Big\{\int_{-\pi/2}^{\pi/2} \Big[\,\boldsymbol{\alpha}(\theta(w))\otimes\boldsymbol{N}\big(\boldsymbol{\alpha}(\theta(w))\big)\otimes\boldsymbol{\alpha}(\theta(w))\,\Big]\ \mathrm{d}w\Big\} : \boldsymbol{\mathcal{C}} \end{aligned} \tag{49}$$

having set $\bar{\boldsymbol{x}} = y\big(\, a_1 \cos\gamma, a_2 \sin\gamma \,\big)$, $\boldsymbol{\alpha}(\theta) = \big(\, a_1^{-1}\cos(\theta+\gamma), a_2^{-1}\sin(\theta+\gamma) \,\big)$, while the function $\theta(w)$ in the second integral is defined implicitly by $\sin\theta = \sqrt{1-y^{-2}}\sin w$.

Isotropic background material, circular inclusion. The exterior Eshelby tensor for a circular inclusion of unit radius is then found, for example by analytical evaluation of (49) using (47), to have the following closed-form expression (with all indices ranging in $\{1,2\}$):

$$\begin{aligned} 2(1-\nu)\mathcal{S}^{\text{ext}}_{ijk\ell}(\bar{\boldsymbol{x}}) = {} & \Big[\, \frac{6}{\bar{x}^8} - \frac{4}{\bar{x}^6} \,\Big] x_i x_j x_k x_\ell + \Big[\, \frac{1}{\bar{x}^4} - \frac{1}{\bar{x}^6} \,\Big] \delta_{ij} x_k x_\ell + \Big[\, \frac{1-2\nu}{\bar{x}^4} - \frac{1}{\bar{x}^6} \,\Big] \delta_{k\ell} x_i x_j \\ & + \Big[\, \frac{\nu}{\bar{x}^4} - \frac{1}{\bar{x}^6} \,\Big] (\delta_{ik} x_j x_\ell + \delta_{jk} x_i x_\ell + \delta_{i\ell} x_j x_k + \delta_{j\ell} x_i x_k) \\ & + \Big[\, \frac{1}{4\bar{x}^4} - \frac{1-2\nu}{2\bar{x}^2} \,\Big] \delta_{ij}\delta_{k\ell} + \Big[\, \frac{1}{4\bar{x}^4} + \frac{1-2\nu}{2\bar{x}^2} \,\Big] (\delta_{ik}\delta_{j\ell} + \delta_{jk}\delta_{i\ell}), \end{aligned} \tag{50}$$

5 Numerical examples

The finite element analysis for each of the following 2D and 3D test cases was carried out with the software Freefem++ [20]. The finite elements for the displacement and adjoint state where chosen as Lagrange $\mathbb{P}^1$ elements on a triangular and tetrahedral mesh, respectively. The mesh of the surface of a human femur was obtained from the mesh database of the GAMMA project [28], while its inner tetrahedral mesh and the surface mesh adaptation were generated thanks to TetGen [43] and FreeYams [21], respectively. The plot of the 2D, 3D functions and meshes was done with Medit [36].

The term in the topological derivative (28) involving an integral on $\mathbb{R}^3 \setminus \mathcal{B}$ was evaluated using (43) and two quadrature rules, namely a 4-point Gauss-Legendre rule on $t \in [0,1]$ and a 26-point Lebedev rule [32] on $\hat{\boldsymbol{y}} \in S^2$ (Sec. 5.2), while two Gauss-Legendre quadratures were used for the 2D example of Sec. 5.1. The known analytical expression (48) of the 3D isotropic exterior Eshelby tensor $\boldsymbol{\mathcal{S}}^{\text{ext}}$ for the unit sphere was directly applied (Secs. 5.1 and 5.2) to avoid additional numerical quadrature work. The examples of Sec. 5.3 rely instead on the special cases (40) and (41) of $\mathrm{D}J$, avoiding both the numerical quadrature in (43) and the recourse to $\boldsymbol{\mathcal{S}}^{\text{ext}}$.

Since the topological derivative depends on the derivatives of $\boldsymbol{u}$ and $\boldsymbol{p}$, the finite element representation of $\mathrm{D}J(\boldsymbol{z})$ is $\mathbb{P}^0$ (piecewise constant). To facilitate graphical post-processing, a regularized version $\mathrm{D}J_r$ of $\mathrm{D}J$ was computed, by applying a standard regularization procedure consisting in solving the variational problem

$$\int_\Omega \big(\, \mathrm{D}J_r\, w + \epsilon \nabla \mathrm{D}J_r \cdot \nabla w \,\big)\, \mathrm{d}V = \int_\Omega \mathrm{D}J\, w\, \mathrm{d}V, \qquad \forall w \in H^1(\Omega).$$

The parameter ϵ controls the diffusion and regularization of $\mathrm{D}J$, at a slight expense of accuracy. For this study ϵ was set to $\epsilon = 10^{-6}$.

5.1 Sensitivity analysis of the Hill-Tsai failure criterion

Composite materials are quite popular in industry thanks to their low weight, high fatigue resistance and good endurance against corrosion. The elastic constitutive relation for such materials, restricted for two-dimensional problems to the in-plane components of the stress

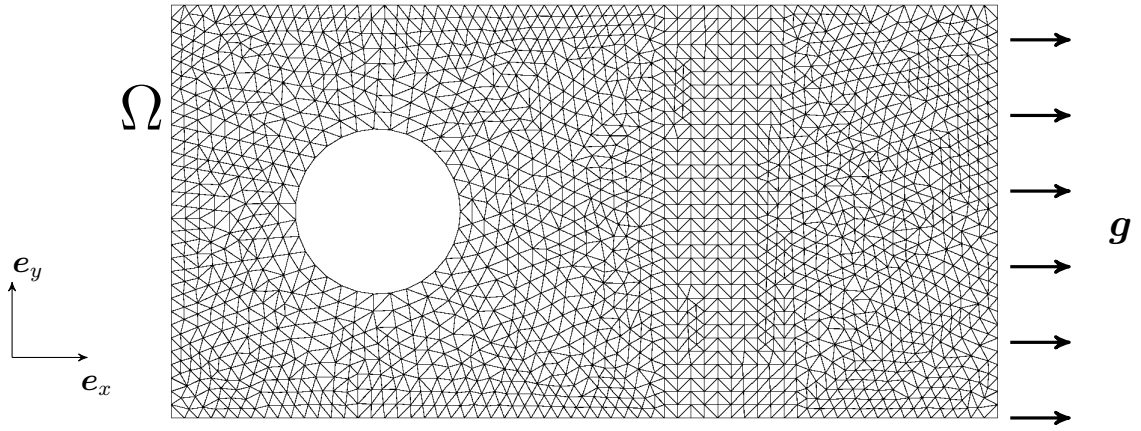

Figure 2: Orthotropic ply Ω clamped to a circular support: configuration and mesh ($\sim 3,700$ elements). A horizontal uniform load $\boldsymbol{g}$ is applied on its right side.

tensor, may be conveniently written in the principal orthotropy directions, and using the Voigt notation, in the form

$$\begin{Bmatrix} \sigma_\ell \\ \sigma_t \\ \tau_{\ell t} \end{Bmatrix} = \frac{1}{1-\nu_{\ell t}\nu_{t\ell}} \begin{bmatrix} E_\ell & \nu_{t\ell}E_\ell & 0 \\ \nu_{\ell t}E_t & E_t & 0 \\ 0 & 0 & 2G_{\ell t} \end{bmatrix} \begin{Bmatrix} \varepsilon_\ell \\ \varepsilon_t \\ \varepsilon_{\ell t} \end{Bmatrix}$$

where the stresses are denoted as σ_ℓ in the fiber direction, σ_t in the direction transverse to the fibers, and $\tau_{\ell t}$ for the shear stresses. This model involves four independent elastic constants, since one must have $\nu_{t\ell}E_\ell = \nu_{\ell t}E_t$.

The Hill-Tsai failure criterion, suitable for orthotropic materials, is an adaptation of the von Mises yield criterion whereby the material strength depends on the direction, according to the orientation of the fiber reinforcement. This criterion can be written as [23]

$$\alpha^2(\boldsymbol{\sigma}) := \frac{\sigma_\ell^2}{\hat{\sigma}_\ell^2} + \frac{\sigma_t^2}{\hat{\sigma}_t^2} - \frac{\sigma_\ell \sigma_t}{\hat{\sigma}_\ell^2} + \frac{\tau_{\ell t}^2}{\hat{\tau}_{\ell t}^2} < 1, \tag{51}$$

where $\hat{\sigma}_\ell$, $\hat{\sigma}_t$ and $\hat{\tau}_{\ell t}$ denote known rupture strengths.

Unlike their metal counterparts, composite structures are incapable to conduct away the extreme electrical currents and electromagnetic fields generated by lighting strikes. Hence the need for protection of composite structures has prompted the development of specialized lighting strike protection materials [22]. An example of such material features metallic parts of conductive material added into the laminate. This numerical example examines, by means of the topological derivative, the sensitivity of the Hill-Tsai criterion (51) to the addition of small metallic inhomogeneities to the orthotropic material, so as to determine (and avoid) those locations for which this material addition make the laminate most vulnerable to failure.

Let the domain $\Omega = \{(x, y) \in (0, 2) \times (0, 1)\} \subset \mathbb{R}^2$ be occupied by a rectangular carbon/epoxy fiber ply (i.e. a composite membrane, with fiber direction $\boldsymbol{e}_\ell = (\boldsymbol{e}_x + \boldsymbol{e}_y)/\sqrt{2}$ and 60% fiber volume fraction), clamped to a circular support. An uniform horizontal tensile traction $\boldsymbol{g} = 10^{-5}E_\ell \boldsymbol{e}_x$ is applied on its right side (Fig. 2).

The elastic parameters of the composite ply are $E_\ell = 135\,\text{GPa}$, $E_t = 10\,\text{GPa}$, $G_{\ell t} = 5\,\text{GPa}$, $\nu_{\ell t} = 0.3$, while the ultimate tensile failure strengths involved in the criterion (51) are

$\hat\sigma_\ell = 1500\,\text{MPa}$, $\hat\sigma_t = 50\,\text{MPa}$, $\hat\tau_{\ell t} = 70\,\text{MPa}$. The metallic inclusions are considered circular and made of aluminum, whose isotropic elastic characteristics are $E = 72\,\text{GPa}$, $\nu = 0.34$, while the von Mises yield strength is $\hat\sigma = 20\text{MPa}$.

Let the densities $\psi, \psi^\star$ entering the definition (23) of the cost functional $J(\mathcal{C}_a)$ be given, in terms of the penalization function Ψ_n introduced in (26), by

$$\psi(\boldsymbol{d}) = \Psi_n\big(\,\alpha^2(\mathcal{C}:\boldsymbol{d})\,\big), \qquad \psi^\star(\boldsymbol{d}) = \Psi_n\big(\,\alpha_\star^2(\mathcal{C}^\star:\boldsymbol{d})\,\big) \tag{52}$$

(with $n \geq 1$). The function α for the composite membrane is given by (51). The corresponding function $\alpha_\star$ for the aluminum is also taken of the form (51) with $\hat\sigma_\ell = \hat\sigma_t = \hat\sigma$ and $\hat\tau_{\ell t} = \hat\sigma/\sqrt{3}$, as this choice reduces the Hill-Tsai criterion to the plane-stress von Mises criterion for isotropic materials. With this choice, $J(\mathcal{C}_a)$ is always nonnegative; moreover, in the limit $n \to \infty$, $J(\mathcal{C}_a) = 0$ unless the threshold (51) is violated at some location. The value $n = 5$ is used in the numerical experiments to follow. The topological derivative $\mathrm{D}J$ is given by (28), with

$$\mathcal{G}(\boldsymbol{z}, \boldsymbol{d}) = \psi(\boldsymbol{\nabla u}(\boldsymbol{z}) + \boldsymbol{d}) - \psi(\boldsymbol{\nabla u}(\boldsymbol{z})) - \partial_d\psi(\boldsymbol{\nabla u}(\boldsymbol{z})):\boldsymbol{d}, \tag{53}$$

and with $\mathcal{G}^\star$ similarly defined in terms of $\psi^\star$. The derivative $\partial_d\psi$ is found to be given by

$$\partial_d\psi(\boldsymbol{\nabla u}):\boldsymbol{d} = \big[\ \big(1 + \alpha^{2n}(\mathcal{C}:\boldsymbol{\nabla u})\big)^{(1-n)/n}\,\alpha^{2(n-1)}(\mathcal{C}:\boldsymbol{\nabla u})\ \big]\,\partial_d\alpha^2(\mathcal{C}:\boldsymbol{\nabla u}):\boldsymbol{d} \tag{54}$$

where, since $\alpha^2(\boldsymbol{\sigma})$ is a symmetric quadratic form in $\boldsymbol{\sigma}$,

$$\partial_d\alpha^2(\mathcal{C}:\boldsymbol{\nabla u}):\boldsymbol{d} = \tfrac{1}{2}\alpha^2\big(\mathcal{C}:(\boldsymbol{\nabla u}(\boldsymbol{z}) + \boldsymbol{d})\big) - \tfrac{1}{2}\alpha^2\big(\mathcal{C}:(\boldsymbol{\nabla u}(\boldsymbol{z}) - \boldsymbol{d})\big).$$

Numerical assessment of the topological derivative evaluation. To provide a validation of expression (28) of $\mathrm{D}J$, the Hill-Tsai cost functional $J(\mathcal{C}_a)$ defined by (23) and (52) is numerically evaluated (with n =1, 2 or 4) for a circular inclusion of finite radius a, centered at $(x, y) = (1,\, 2/3)$. The mesh (Fig. 3) was designed to allow considering several values of a, i.e. a sequence of nested concentric inclusions. The discrepancy $e(a)$ between $J(\mathcal{C}_a)$ evaluated either numerically or using (28), defined by

$$e(a) := \frac{|J(\mathcal{C}_a) - J(\mathcal{C}) - a^2\mathrm{D}J(\boldsymbol{z})|}{|a^2\mathrm{D}J(\boldsymbol{z})|}, \qquad \text{with } \Delta J := J(\mathcal{C}_a) - J(\mathcal{C})$$

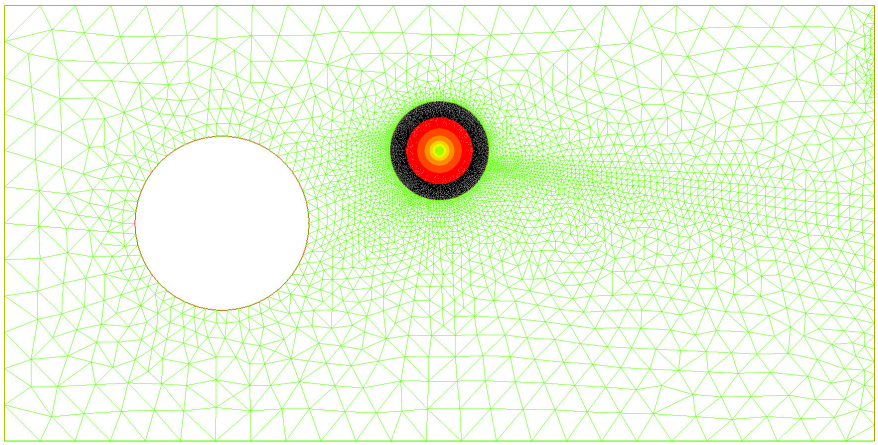

Figure 3: Orthotropic ply: mesh for the numerical validation of $\mathrm{D}J$.

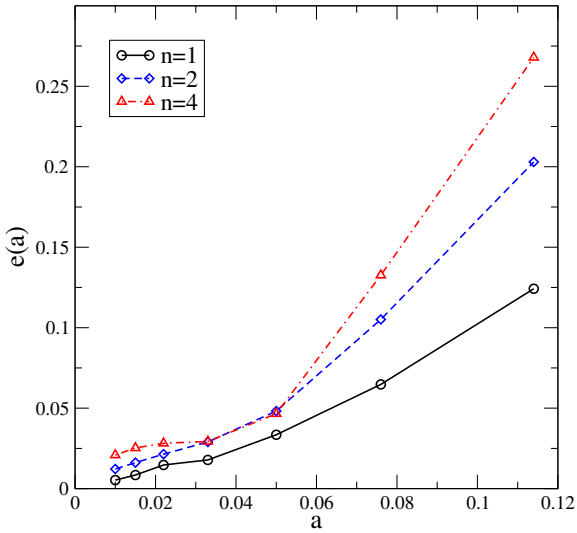

Figure 4: Orthotropic ply: numerical validation of $\mathrm{D}J$ for nested inclusions.

is plotted against a in Fig. 4. A numerical test of correctness of the evaluation of $\mathrm{D}J(\boldsymbol{z})$ then consists in checking that $e(a) = o(a)$ for small a. This desired trend is achieved in Fig. 4.

Topological derivative distribution in the composite membrane. Figure 5 shows the distributions of values of the Hill-Tsai criterion (51) and its topological derivative. The metallic inclusion should not be placed in zones where $\mathrm{D}J$ takes higher values.

5.2 Sensitivity of the von Mises criterion for an isotropic 3D beam

Consider a beam occupying the domain $\Omega = \{\,(x,y,z) \in (-0.1,0.1)\times(-0.5,0.5)\times(-0.1,0.1)\,\}$, clamped on its rear face $y = -0.5$, made of an isotropic elastic material (Fig. 6). A traction $\boldsymbol{g} = x\boldsymbol{e}_z$ is applied on the front face, so as to produce torsion around the main axis $x = z = 0$. The remaining faces are traction-free.

The beam is meshed with $\sim 75,500$ tetrahedral elements and the isotropic elastic properties of the material are normalized and given as Young's modulus $E = 1$ and Poisson's ratio

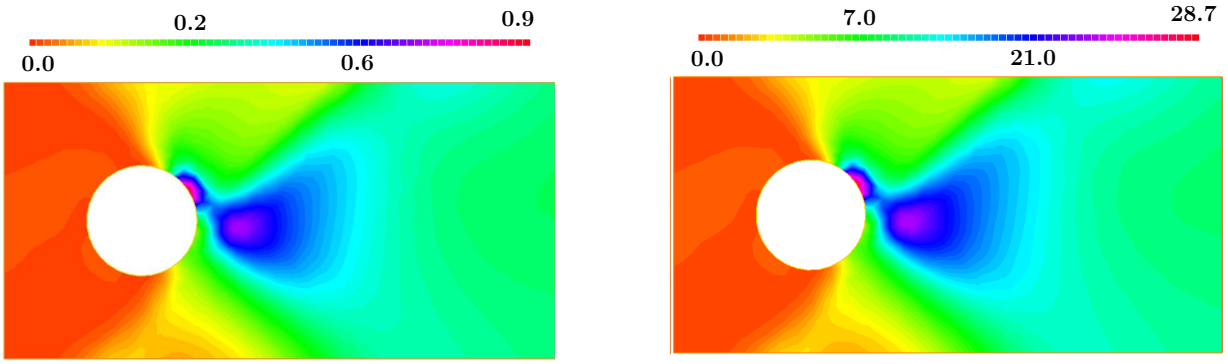

(a) Values of the Hill-Tsai failure criterion

(b) Values of the topological derivative

Figure 5: Orthotropic ply: sensitivity analysis of the Hill-Tsai failure criterion.

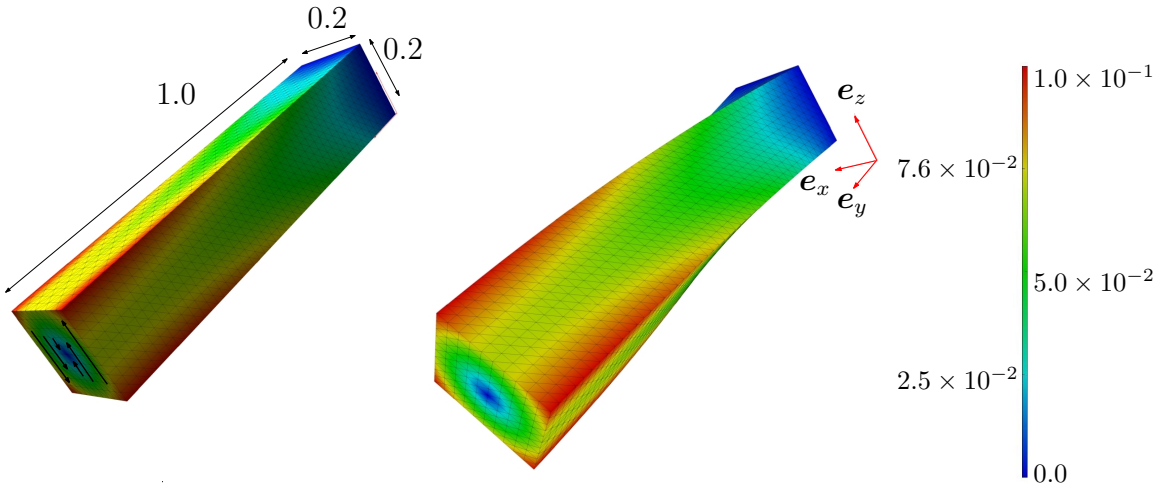

Figure 6: Beam under torsion: geometrical configuration, with color scale of displacement modulus (undeformed and deformed views)

$\nu = 0.3$. We study the variation of the von Mises criterion when a small spherical cavity is introduced in the beam. This is a typical example of sensitivity analysis for topology optimization. The von Mises yield criterion sets a threshold on the *equivalent stress* σ_{eq}:

$$\alpha(\boldsymbol{\sigma}) \leq 1, \qquad \text{with} \quad \alpha(\boldsymbol{\sigma}) := \sigma_{\text{eq}}/\hat{\sigma}, \quad \sigma_{\text{eq}} := \left(\tfrac{3}{2}\text{dev}(\boldsymbol{\sigma}) : \text{dev}(\boldsymbol{\sigma})\right)^{1/2}, \tag{55}$$

where $\text{dev}(\boldsymbol{\sigma}) := \boldsymbol{\sigma} - \frac{1}{3}\text{tr}(\boldsymbol{\sigma})\boldsymbol{I}$ is the deviatoric stress tensor and $\hat{\sigma}$ is a critical stress threshold for the material, here chosen as $\hat{\sigma} = 0.1$. Under the given torsional loading, the stress state then satisfies (55) in the entire beam (see Figure 7).

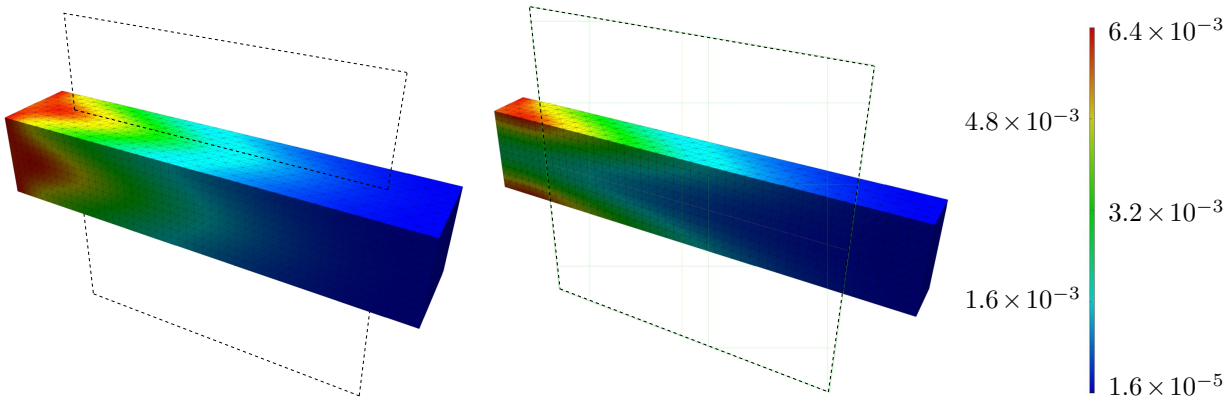

Figure 7: Beam under torsion: contour plot of $2\sigma_{eq}^2/3 = |\text{dev}(\boldsymbol{\sigma})|^2$ on the boundary (left) and inside the beam along a transversal cut (right).

Considering σ_{eq} as a function of the displacement gradient through the elastic constitutive equation $\boldsymbol{\sigma} = \boldsymbol{\mathcal{C}} : \boldsymbol{\nabla u}$, and given that the trial cavity B_a contains no material (i.e. $\boldsymbol{\mathcal{C}}^\star = \boldsymbol{0}$), ψ and $\psi^\star$ are chosen as

$$\psi(\boldsymbol{\nabla u}) = \Psi_n\big(\alpha^2(\boldsymbol{\mathcal{C}} : \boldsymbol{d})\big), \quad \psi^\star(\boldsymbol{d}) = 0 \tag{56}$$

where Ψ_n is again the penalty function (26), with $n \geq 1$ and α is defined by (55). Then if $n \to \infty$, the value of the integral of (56) on Ω is nonzero only if (55) is violated in some part of

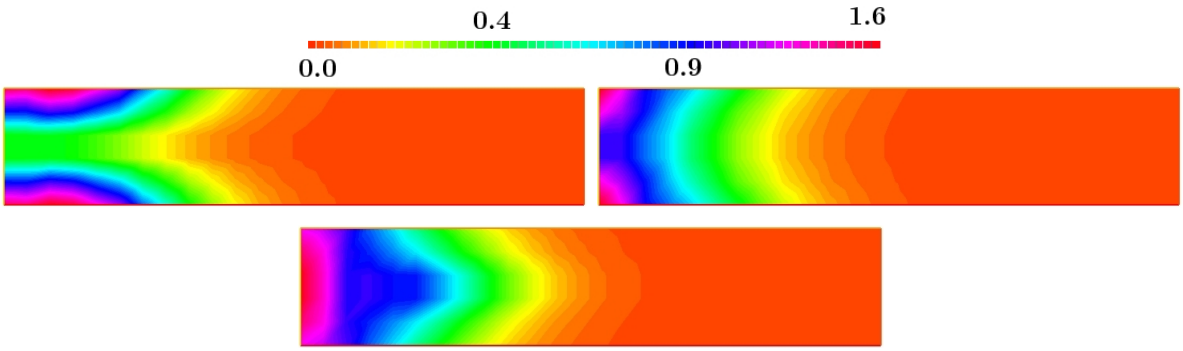

Figure 8: Beam under torsion: color maps of $|\mathrm{D}J|$ in planes $x = 0$ (top left), $x = 0.05$ (top right) and $x = 0.1$ (bottom). The left boundary corresponds to the clamped face of the beam.

the domain. Let us take e.g. $n = 5$. Thus, noting that $\Delta\psi = -\psi$, the topological derivative of the functional

$$J_a(\boldsymbol{\mathcal{C}}_a) = \mathbb{J}_a(\boldsymbol{\nabla u}_a) = \int_{\Omega\setminus B_a} \psi(\boldsymbol{\nabla u}_a)\,\mathrm{d}V$$

is given by

$$\begin{aligned}\mathrm{D}J(\boldsymbol{z}) = &-|\mathcal{B}|\psi(\boldsymbol{\nabla u}(\boldsymbol{z})) - \boldsymbol{\nabla p}(\boldsymbol{z}) : \boldsymbol{\mathcal{A}} : \boldsymbol{\nabla u}(\boldsymbol{z}) + \partial_d\psi(\boldsymbol{\nabla u}(\boldsymbol{z})) : |\mathcal{B}|\boldsymbol{\nabla v}_{\mathcal{B}}[\boldsymbol{\nabla u}(\boldsymbol{z})] \\ &+ \int_{\mathbb{R}^3\setminus\mathcal{B}} \mathcal{G}(\boldsymbol{z}, \boldsymbol{\nabla v}_{\mathcal{B}}[\boldsymbol{\nabla u}(\boldsymbol{x})])(\bar{\boldsymbol{x}})\,\mathrm{d}V,\end{aligned}$$

where $\mathcal{G}(\boldsymbol{z}, \boldsymbol{d})$ again has the form (53), this time with ψ defined by (56) and (55). The derivative ∂_d still has the form (54), now with

$$\partial_d\alpha^2(\boldsymbol{\mathcal{C}} : \boldsymbol{\nabla u}) : \boldsymbol{d} = \frac{3}{\hat{\sigma}^2}\mathrm{dev}(\boldsymbol{\mathcal{C}} : \boldsymbol{\nabla u}) : \mathrm{dev}(\boldsymbol{\mathcal{C}} : \boldsymbol{d})$$

The distribution of the values of $\mathrm{D}J$ for three different cut planes is plotted in Figure 8. The generation of these three planar isosurface maps entailed, for each evaluation point $\boldsymbol{z}$, the evaluation of (43) via numerical quadrature (see the opening part of this section) and in practice required about 1 mn of CPU time on a desktop PC. This shows the practical feasibility of generating topological derivative maps even for the non-quadratic case and under 3D conditions.

Remark 6. *The similarities between the distribution of $|\boldsymbol{\sigma}_{dev}|$ in Figure 7 and the topological derivative in Figure 8 are noticeable. This observation supports the idea of using $|\boldsymbol{\sigma}|$ as a sensitivity measure for topology optimization. In fact this property is exploited by evolutionary algorithms [25] and soft kill option algorithms [9] for lightweight design subjected to a yield criterion. In general, these algorithms search the optimal topology through a fully stressed design, by gradually removing the low stressed material w.r.t. a certain reference value.*

5.3 3D anisotropic non-destructive testing

Two applications of non-destructive control in anisotropic materials are now presented, one pertaining to medical imaging and the other to composite structures. Indeed, several groups

have recently investigated the topological derivative as a means for imaging hidden flaws, see for instance [3, 48], and also [45] for an application on experimental data. Existing investigations in this direction are based on usual displacement-based cost functionals (typically of the output least-squares type). In contrast, we examine in this example an alternative approach where the misfit to experimental data is formulated in terms of an energy (and hence strain- or stress-based) cost functional. Assuming the availability of a displacement measurement $\boldsymbol{u}_0$ over a part ω of the elastic solid Ω, using e.g. full-field kinematical data [10], the strain energy of the measurement misfit is given by

$$J_\omega(\boldsymbol{\mathcal{C}}_a) = \mathbb{J}_a(\boldsymbol{\nabla u}_a; \omega) = \int_\omega \boldsymbol{\nabla}(\boldsymbol{u}_a - \boldsymbol{u}_0) : \boldsymbol{\mathcal{C}}_a : \boldsymbol{\nabla}(\boldsymbol{u}_a - \boldsymbol{u}_0)\, \mathrm{d}V. \tag{57}$$

Depending on whether the trial inhomogeneity B_a is located inside or outside of ω, we distinguish two cases:

1. $B_a \subset \omega$. This case is relevant when complete displacement measurements are available over a particular region ω inside Ω. Adapting (41), the topological derivative reads

$$\mathrm{D}J(\boldsymbol{z}) = |\mathcal{B}| \boldsymbol{\nabla u}_0(\boldsymbol{z}) : \Delta\boldsymbol{\mathcal{C}} : \boldsymbol{\nabla u}_0(\boldsymbol{z}) - \boldsymbol{\nabla}(\boldsymbol{p} + 2\boldsymbol{u}_0 - \boldsymbol{u}) : \boldsymbol{\mathcal{A}} : \boldsymbol{\nabla u} \qquad (\boldsymbol{z} \in \omega),$$

   where the adjoint solution $\boldsymbol{p}$ satisfies the variational formulation

$$\big\langle \boldsymbol{p}, \boldsymbol{w} \big\rangle_\Omega^{\mathcal{C}} = 2 \big\langle \boldsymbol{u} - \boldsymbol{u}_0, \boldsymbol{w} \big\rangle_\omega^{\mathcal{C}}, \qquad \forall \boldsymbol{w} \in W_0(\Omega).$$

2. $B_a \subset \Omega \setminus \bar{\omega}$. The interest of this situation is justified when we have a set of small control volumes inside a body and we want to identify the position of the anomaly outside the measured volumes. As previously seen in Section 3.2, there is no second order contribution in the topological derivative and $\mathrm{D}J$ simply reads

$$\mathrm{D}J(\boldsymbol{z}) = -\boldsymbol{\nabla p}(\boldsymbol{z}) : \boldsymbol{\mathcal{A}} : \boldsymbol{\nabla u}(\boldsymbol{z}) \qquad (\boldsymbol{z} \in \Omega \setminus \bar{\omega}).$$

First application. It is concerned with the detection of anomalous femoral bone tissue. The local change of elastic properties in femoral bone may be provoked e.g. by cancer metastasis, traumatic or pathological fractures. Moreover, bone cell elasticity and morphology changes during the cell cycle [29], and elasticity differences between cancerous and healthy tissues of various kinds have been experimentally established [30, 42].

Additionally, bone is a complex material, with a multiphasic, heterogeneous and anisotropic microstructure [17]. In particular, femoral bone can be accurately modelled a transversely isotropic material whose principal orientations are defined based either on the trabecular structures or the harvesian system, according to whether the bone is cancellous or cortical [47].

Consider the proximal part Ω of a femoral bone (Fig. 9), contained in the box $\big\{ (x, y, z) \in (0.03, 0.09) \times (0.04, 0.08) \times (0.01, 0.11) \big\}$ and meshed with $\sim 213,600$ tetrahedral elements (mesh size $h = 0.001$). The elastic properties of the healthy bone are by simplification assumed to be homogeneous and transversely isotropic, with normalized elastic constants given by

$$E_x = E_y = 0.5, \quad E_z = 1, \quad \nu_{xy} = \nu_{xz} = \nu_{yz} = 0.35, \quad G_{xz} = G_{yz} = 0.03.$$

The anomalous tissue is assumed to be a small and stiffer spherical inhomogeneity (Fig. 10) with radius 0.005 and center at $(0.05, 0.06, 0.06)$. Its Young and shear moduli are twice those of the healthy bone, while both materials have the same Poisson ratios. The bone is clamped at $z = 0.01$ and loaded with a vertical force density $\boldsymbol{g} = -1 \times 10^{-3} \boldsymbol{e}_z$ applied on the top surface of the femur ($z \in [0.10, 0.11]$).

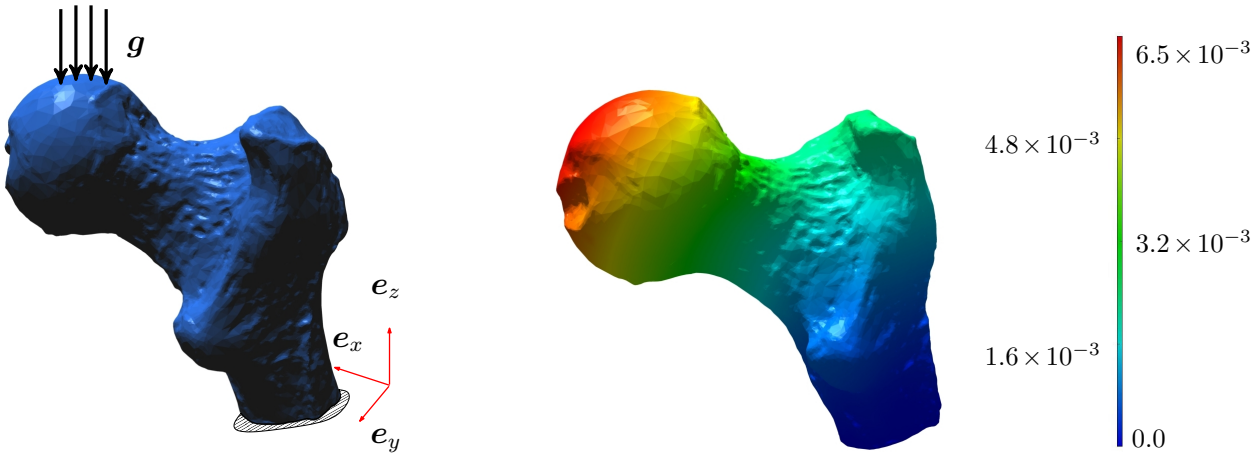

Figure 9: Femoral bone: a uniform vertical load $\boldsymbol{g} = -10^{-3}\boldsymbol{e}_z$ is applied on the head of the femur (simulating the body weight) while the distal horizontal section $z = 0.01$ is clamped (left). The right panel shows a color scale of the displacement modulus.

The measurement region ω is defined as the vertically central zone of the femur (shown in red in Fig. 10). Simulated data is assumed to be exact for simplicity. While this constitutes a strong idealization, previous numerical experiments on flaw identification by topological derivative have shown the approach to be only moderately sensitive to measurement noise [11].

Figure 11 shows three iso-surfaces of $\mathrm{D}J$ with decreasing levels $\eta \approx -0.19$ (yellow), $\eta \approx -0.45$ (green) and $\eta \approx -0.71$ (blue), where an iso-surface S_η with level η relative to the (negative) absolute minimum $\mathrm{D}J_{\min} := \min_{\boldsymbol{z}\in\Omega} \mathrm{D}J(\boldsymbol{z})$ is defined by

$$S_\eta = \left\{ \boldsymbol{z} \in \Omega, \mathrm{D}J(\boldsymbol{z}) = \eta |\mathrm{D}J_{\min}| \right\} \tag{58}$$

Those iso-surfaces show the location of the anomalous tissue to be correctly identified.

Second application. It consists in detecting a failure point leading to damage inside a composite structure. Multi-laminate composite structures are made of multiple orthotropic

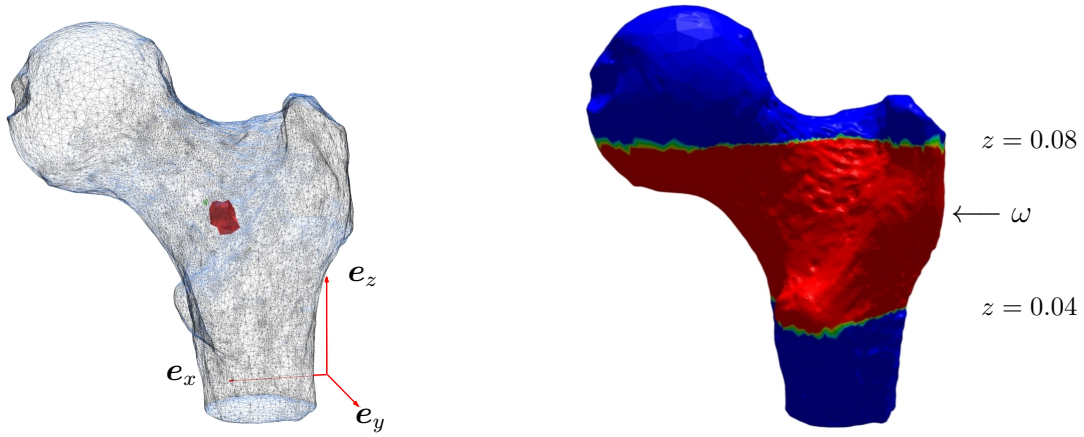

Figure 10: Femoral bone: anomalous tissue (left, in red) and measurement region ω (right, in red).

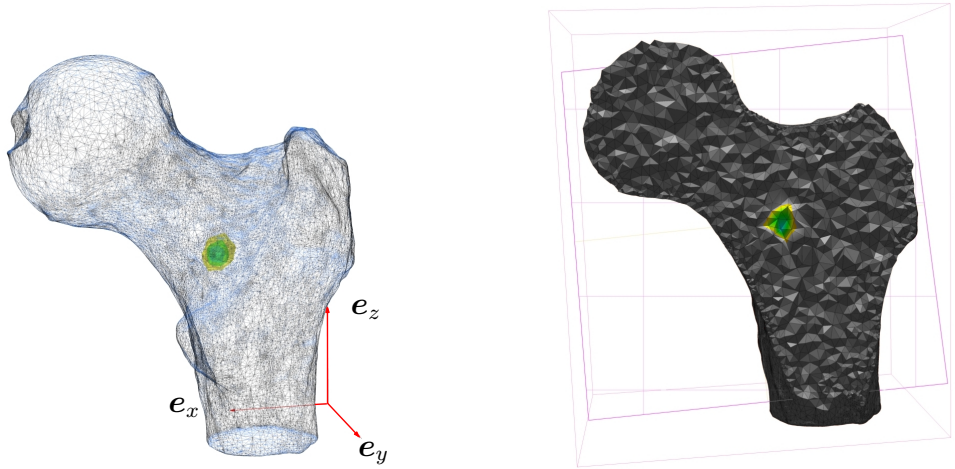

(a) Three-dimensional view. **(b)** Transversal cut view.

Figure 11: Femural bone: iso-surfaces $\eta \approx -0.19$ (yellow), $\eta \approx -0.45$ (green) and $\eta \approx -0.71$ (blue) of DJ.

plies, each of them composed of a weak matrix (most often polymeric) and reinforcement fibers (carbon, glass, kevlar, etc). The main failure modes in composites are fiber rupture, matrix rupture and delamination [23]. We consider here a composite cube $\Omega = \{(x, y, z) \in (0, 0.2)^3\}$, filled up with $\sim 23,000$ tetrahedral elements (mesh size $h = 0.011$), made of three stacked layers of equal thickness (Fig. 12) whose constitutive elastic properties are transversely isotropic. The normalized elastic constants for the bottom layer are

$$E_x = 1 \ , E_y = E_z = 0.05, \quad \nu_{xy} = \nu_{xz} = \nu_{yz} = 0.35, \quad G_{xz} = G_{yz} = G_{xy} = 0.03,$$

The middle and top layers have the same elastic constants than the lowest one, but with the horizontal principal orthotropy directions resulting from a 45^o and 90^o rotation of the

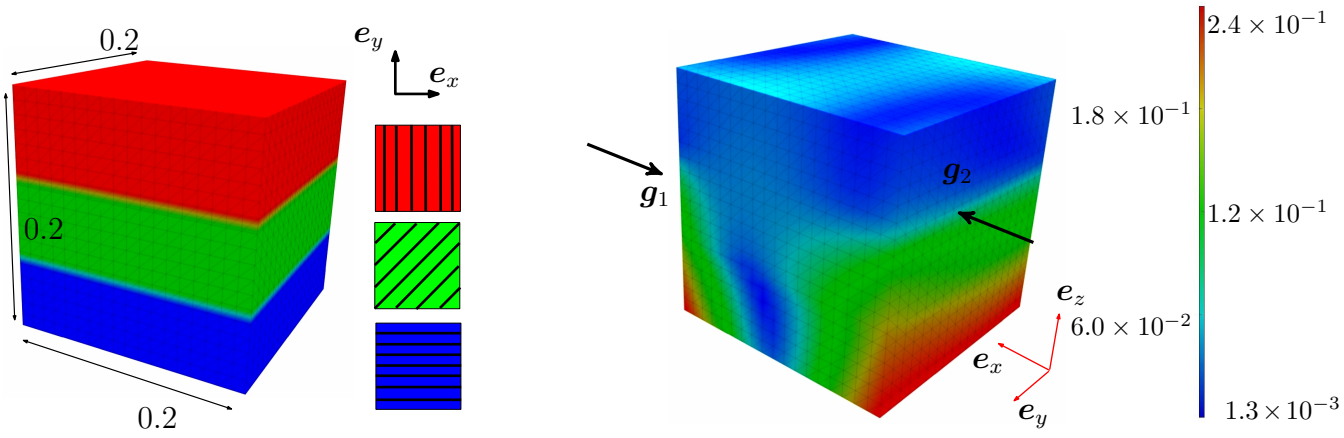

(a) Layered cube, and fiber orientation. **(b)** A color scale of the displacement modulus.

Figure 12: Layered cube: two uniform compression loads $\boldsymbol{g}_1 = -0.1\boldsymbol{e}_x$ and $\boldsymbol{g}_2 = 0.1\boldsymbol{e}_x$ are respectively applied on the faces of the cube $x = 0.2$ and $x = 0$. Displacements are not affine in the spatial coordinates due to the anisotropy.

x, y axes, respectively. The failure point is modeled as a spherical inhomogeneity, of centre $(0.1, 0.15, 0.1)$ and radius 0.01, and with very low elastic moduli properties $\boldsymbol{\mathcal{C}}^\star = 10^{-5}\boldsymbol{\mathcal{C}}$. The considered misfit criterion is again of the form (57), this time with the measurement region ω consisting of a set of M small disconnected control volumes: $\omega = \cup\omega_j$ $(1 \le j \le M)$, with $\omega_j \subset \Omega$ and $\overline{\omega}_i \cap \overline{\omega}_j = \emptyset$ (two such configurations, with $M = 44$ and $M = 729$, are shown on Fig. 13). The adjoint solution $\boldsymbol{p}$ in this case solves

$$\int_\Omega \boldsymbol{\nabla p} : \boldsymbol{\mathcal{C}} : \boldsymbol{\nabla q} \, \mathrm{d}V = 2 \sum_{i=1}^{M} \int_{\omega_i} \boldsymbol{\nabla}(\boldsymbol{u} - \boldsymbol{u}_0) : \boldsymbol{\mathcal{C}} : \boldsymbol{\nabla q} \, \mathrm{d}V, \qquad \forall \boldsymbol{q} \in W_0(\Omega).$$

Fig. 14 shows one iso-surface (in green) of $\mathrm{D}J$ with negative level surrounding the minimum of $\mathrm{D}J(\boldsymbol{z})$ for each control volume configuration of Figure 13 (with $\eta \approx -0.65$ and $\eta \approx -0.3$, respectively). As expected, the identification quality improves with the number of measurement zones. Moreover, the absolute minima of $\mathrm{D}J$ are found to be $\mathrm{D}J_{\min} \approx -1.3{\times}10^{-3}$ and $\mathrm{D}J_{\min} \approx -6.9 \times 10^{-2}$, respectively, which is another indication of configuration 2 being more sensitive to a small defect.

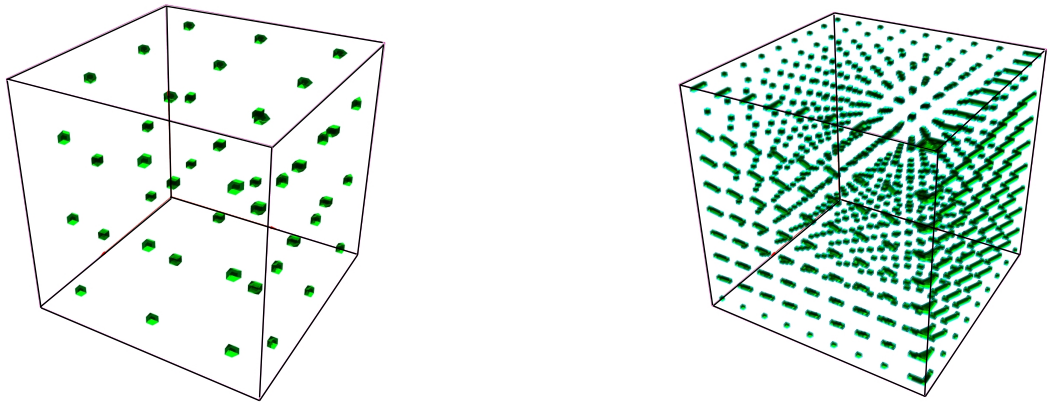

(a) Configuration 1 $(M = 44)$. **(b)** Configuration 2 $(M = 729)$.

Figure 13: Layered cube: control volumes ω_j $(1 \le j \le M)$.

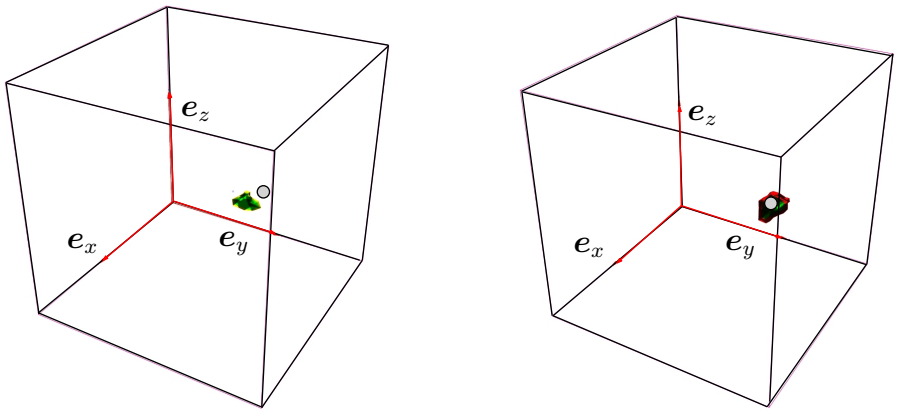

(a) Configuration 1 $(M = 44)$. **(b)** Configuration 2 $(M = 729)$.

Figure 14: Layered cube: iso-surface S_η with $\eta \approx -0.65$ (left) and $\eta \approx -0.3$ (right) of $\mathrm{D}J$. The grey sphere shows the correct location of the failure point.

6 Conclusion

The topological derivative $\mathrm{D}J$ of a general cost functional J depending on both the displacement and its gradient (i.e. on the stress, assuming linear elastic constitutive properties) has been established by means of a rigorous small-inhomogeneity asymptotic expansion, under arbitrary 3D anisotropic conditions. This generalized version of $\mathrm{D}J$ combines the previously-known terms associated with the topological derivative of displacement-based functionals and new terms which arise only for the case of stress-dependent functionals. Furthermore, our result holds for the case of a trial inclusions B_a appearing either inside or outside the support $\omega \subset \Omega$ of the volume density ψ_a of the functional J (i.e. only the more-complex case case where B_a sits on $\partial\omega$ is left out). From a computational standpoint, one of the new terms in $\mathrm{D}J$ entails carrying out a numerical integration on the unbounded region $\mathbb{R}^3 \setminus \mathcal{B}$, and a suitable change of variables allowing subsequent use of standard quadrature formulas was given for both the 3D and 2D cases. Moreover, the computational procedure involves both the exterior and interior Eshelby tensors, for which explicit formulas are available in a few cases, and which can otherwise be evaluated by numerical quadrature of integral representation formulas such as (46). Numerical examples demonstrate both the feasibility and usefulness of computing the field $\boldsymbol{z} \to \mathrm{D}J(\boldsymbol{z})$, even for the case of non-quadratic stress-based functionals for three-dimensional configurations for which substantial numerical quadrature work is necessary.

References

[1] Allaire, G., de Gournay, F., Jouve, F., Toader, A.-M.. Structural optimization using topological and shape sensitivity via a level-set method. *Control and Cybernetics*, **34**:59–80 (2005).

[2] Allaire, G., Jouve, F., Van Goethem, N. Damage and fracture evolution in brittle materials by shape optimization methods. *J. Comput. Phys.*, **230**:5010–5044 (2011).

[3] Ammari, H., Bretin, E., Garnier, J., Jing, W., Kang, H., Wahab, A. Localization, stability, and resolution of topological derivative based imaging functionals in elasticity. *arXiv preprint arXiv:1210.6760* (2012).

[4] Ammari, H., Kang, H. *Polarization and moment tensors with applications to inverse problems and effective medium theory*. Applied Mathematical Sciences, Vol. 162. Springer-Verlag (2007).

[5] Ammari, H., Kang, H., Nakamura, G., Tanuma, K. Complete asymptotic expansions of solutions of the system of elastostatics in the presence of an inclusion of small diameter and detection of an inclusion. *J. Elast.*, **67**:97–129 (2002).

[6] Amstutz, S, Andrä, H. A new algorithm for topology optimization using a level-set method. *J. Comput. Phys.*, **216**:573–588 (2006).

[7] Amstutz, S, Novotny, A. A., de Souza Neto, E. A. Topological derivative-based topology optimization of structures subject to Drucker-Prager stress constraints. *Comp. Meth. Appl. Mech. Eng.*, **233**:123–136 (2012).

[8] Amstutz, Samuel, Novotny, Antonio A. Topological optimization of structures subject to Von Mises stress constraints. *Structural and Multidisciplinary Optimization*, **41**(3):407–420 (2010).

[9] Baumgartner, A., Harzheim, L., Mattheck, C. SKO (soft kill option): the biological way to find an optimum structure topology. *Int. J. Fatigue*, **14**:387–393 (1992).

[10] Bay, B. K., Smith, T. S., Fyhrie, D. P., Saad, M. Digital volume correlation: three-dimensional strain mapping using X-ray tomography. *Exp. Mech.*, **39**:217–226 (1999).

[11] Bellis, C., Bonnet, M. A FEM-based topological sensitivity approach for fast qualitative identification of buried cavities from elastodynamic overdetermined boundary data. *Int. J. Solids Struct.*, **47**:1221–1242 (2010).

[12] Bellis, C., Bonnet, M., Cakoni, F. Acoustic inverse scattering using topological derivative of far-field measurements-based L^2 cost functionals. *Inverse Prob.*, **29**:075012 (2013).

[13] Beretta, E., Bonnetier, E., Francini, E., Mazzucato, A. L. Small volume asymptotics for anisotropic elastic inclusions. *Inverse Prob. Imaging*, **6**:1–23 (2011).

[14] Bhargava, R. D., Radhakrishna, H. C. Elliptic inclusion in orthotropic medium. *J. Phys. Soc. Jpn.*, **19**:396–405 (1964).

[15] Bonnet, M., Delgado, G. The topological derivative in anisotropic elasticity. *Quart. J. Mech. Appl. Math.*, **66**:557–586 (2013).

[16] Cedio-Fengya, D. J., Moskow, S., Vogelius, M. Identification of conductivity imperfections of small diameter by boundary measurements. Continuous dependence and computational reconstruction. *Inverse Prob.*, **14**:553–595 (1998).

[17] Doblaré, M., Garcıa, J. M., Gómez, M. J. Modelling bone tissue fracture and healing: a review. *Eng. Frac. Mech.*, **71**:1809–1840 (2004).

[18] Eshelby, J. D. The determination of the elastic field of an ellipsoidal inclusion and related problems. *Proc. Roy. Soc. A*, **241**:376–396 (1957).

[19] Feijóo, G. R. A new method in inverse scattering based on the topological derivative. *Inverse Prob.*, **20**:1819–1840 (2004).

[20] Freefem++. http://www.freefem.org/ff++/ (2013).

[21] Freeyams. *http://www.ann.jussieu.fr/frey/software.html* (2001).

[22] Gardner, G. Lightning strike protection for composite structures. *High Performance Composites*, **14**:44 (2006).

[23] Gay, D., Hoa, S. V., Tsai, S. W. *Composite materials: design and applications*. CRC press (2002).

[24] Gradshteyn, I. S., Ryzhik, I. M. *Tables of integrals, series and products (seventh edition)*. Elsevier (2007).

[25] Hinton, E., Sienz, J. Fully stressed topological design of structures using an evolutionary procedure. *Eng. Comp.*, **12**:229–244 (1995).

[26] Hwu, C., Ting, T. C. T. Two-dimensional problems of the anisotropic elastic solid with an elliptic inclusion. *Quart. J. Mech. Appl. Math.*, **42**:553–572 (1989).

[27] Il'in, A. M. *Matching of asymptotic expansions of solutions of boundary value problems*. American Mathematical Society (1992).

[28] INRIA. 3D research meshes database, Gamma project. *http://www-roc.inria.fr/gamma/gamma/Accueil/* (2012).

[29] Kelly, G. M., Kilpatrick, J. I., Van Es, M. H., Weafer, P. P., Prendergast, P. J., Jarvis, S. P. Bone cell elasticity and morphology changes during the cell cycle. *J. Biomech.*, **44**:1484–1490 (2011).

[30] Krouskop, T. A., Wheeler, T. M., Kallel, F., Garra, B. S., Hall, T. Elastic moduli of breast and prostate tissues under compression. *Ultrasonic imaging*, **20**:260–274 (1998).

[31] Kupradze, V. D. (ed.). *Three-dimensional problems of the mathematical theory of elasticity and thermoelasticity*. North Holland (1979).

[32] Lebedev, V. I., Laikov, D. N. A quadrature formula for the sphere of the 131st algebraic order of accuracy. *Doklady Mathematics*, **59**(3):477–481 (1999).

[33] Masmoudi, M., Pommier, J., Samet, B. The topological asymptotic expansion for the Maxwell equations and some applications. *Inverse Prob.*, **21**:547–564 (2005).

[34] Maz'ya, V., Nazarov, S. A., Plamenevskii, B. A. *Asymptotic theory of elliptic boundary value problems under a singular perturbation of the domains (vols. 1 and 2)*. Birkhaüser (2000).

[35] McLean, W. *Strongly elliptic systems and boundary integral equations*. Cambridge (2000).

[36] Medit. *http://www.ann.jussieu.fr/frey/software.html* (2001).

[37] Mura, T. *Micromechanics of Defects in Solids*. Martinus Nijhoff (1987).

[38] Nazarov, S. A., Sokolowski, J., Specovius-Neugebauer, M. Polarization matrices in anisotropic heterogeneous elasticity. *Asympt. Anal.*, **68**:189–221 (2010).

[39] Samet, B., Amstutz, S., Masmoudi, M. The topological asymptotic for the Helmholtz equation. *SIAM J. Control Optim.*, **42**:1523–1544 (2004).

[40] Schneider, M., Andrä, H. The topological gradient in anisotropic elasticity with an eye towards lightweight design. *Math. Meth. in Appl. Sc.* (2013, in press).

[41] Sokolowski, Jan, Zochowski, Antoni. On the topological derivative in shape optimization. *SIAM journal on control and optimization*, **37**(4):1251–1272 (1999).

[42] Suresh, S. Nanomedicine: elastic clues in cancer detection. *Nature Nanotechnology*, **2**:748–749 (2007).

[43] Tetgen. *http://wias-berlin.de/software/tetgen/* (2011).

[44] Theocaris, P. S., Ioakimidis, N. I. The inclusion problem in plane elasticity. *Quart. J. Mech. Appl. Math.*, **30**:437–448 (1977).

[45] Tokmashev, R., Tixier, A., Guzina, B. Experimental validation of the topological sensitivity approach to elastic-wave imaging. *Inverse Prob.*, **29**:125005 (2013).

[46] Willis, J. R. Anisotropic elastic inclusion problems. *Quart. J. Mech. Appl. Math.*, **17**:157–174 (1963).

[47] Yang, H.-S., Guo, T.-T., Wu, J.-H., Ma, X. Inhomogeneous material property assignment and orientation definition of transverse isotropy of femur. *J. Biomed. Sc.*, **2**:419–424 (2009).

[48] Yuan, H., Guzina, B. B., Sinkus, R. Application of topological sensitivity toward tissue elasticity imaging using magnetic resonance data. *J. Eng. Mech. ASCE* (2012).

A The 2D plane-strain case

Inclusion and inhomogeneity problems in plane strain have been addressed in many references, with solution methods usually based on complex potentials, see e.g. [14, 26, 44, 46]. Here, we derive the exterior Eshelby tensor $\boldsymbol{\mathcal{S}}^{\text{ext}}(\boldsymbol{x})$ such that the displacement $\boldsymbol{u}(\boldsymbol{x})$ produced in an infinite two-dimensional anisotropic elastic medium by the application of an eigenstrain $\boldsymbol{E}^\star \in \mathbb{R}^{2\times 2}_{\text{sym}}$ in an elliptical region $\mathcal{B}$ satisfies

$$\boldsymbol{\nabla} \boldsymbol{v}_{\mathcal{B}}[\boldsymbol{E}^\star](\boldsymbol{x}) = \boldsymbol{\mathcal{S}}^{\text{ext}}(\boldsymbol{x}) : \boldsymbol{E}^\star \qquad \boldsymbol{x} \in \mathbb{R}^2. \tag{59}$$

The derivation is done by means of a direct evaluation of the integral representation formula of $\boldsymbol{u}(\boldsymbol{x})$, which under the present conditions (anisotropic, plane strain) reads

$$\boldsymbol{u}(\boldsymbol{x}) = \frac{\mathrm{i}}{(2\pi)^2} \Big\{ \int_{\mathbb{R}^2} \int_{\mathcal{B}} \exp(\mathrm{i}\boldsymbol{\eta}\cdot(\boldsymbol{\xi}-\boldsymbol{x})) \boldsymbol{N}(\boldsymbol{\eta}) \otimes \boldsymbol{\eta} \, \mathrm{d}V(\boldsymbol{\xi}) \, \mathrm{d}V(\boldsymbol{\eta}) \Big\} : \boldsymbol{\mathcal{C}} : \boldsymbol{E}^\star \tag{60}$$

The above fourth-dimensional integral over $(\boldsymbol{\xi}, \boldsymbol{\eta}) \in \mathcal{B} \times \mathbb{R}^2$ is now evaluated with the help of coordinate transformations. To this aim, $\mathcal{B}$ is assumed without loss of generality to be centered at the coordinate origin and with its principal directions directed along the coordinate axes. The evaluation point $\boldsymbol{x} \in \mathbb{R}^2$ is parameterized as

$$\boldsymbol{x}(y, \gamma) = y \left(a_1 \cos(\gamma), a_2 \sin(\gamma) \right), \quad \gamma \in [0, 2\pi], y \in (0, \infty), \tag{61}$$

and two mappings are introduced. First, $f: \ (t, \theta) \in \mathbb{R}^+ \backslash \{0\} \times [0, 2\pi[\ \longmapsto \ (\eta_1, \eta_2) \in \mathbb{R}^2 \backslash \{(0,0)\}$ is defined by

$$\begin{cases} \eta_1(t,\theta) = t\alpha_1(\theta) \\ \eta_2(t,\theta) = t\alpha_2(\theta) \end{cases} \qquad \text{with} \quad \boldsymbol{\alpha}(\theta) = (\alpha_1, \alpha_2)(\theta) := \big(a_1^{-1} \cos(\theta+\gamma), a_2^{-1} \sin(\theta+\gamma) \big), \tag{62}$$

which implies

$$\mathrm{d}V(\boldsymbol{\eta}) = (a_1 a_2)^{-1} t \, \mathrm{d}t \, \mathrm{d}\theta,$$

Then, for given $\boldsymbol{\eta} \in \mathbb{R}^2 \setminus \{\boldsymbol{0}\}$ (i.e. for given $(t, \theta) \in \mathbb{R}^+ \setminus \{0\}$), $g: \ (z_1, z_2) \in \mathcal{D} \ \longmapsto \ (\xi_1, \xi_2) \in \mathcal{B}$ (where $\mathcal{D} \subset \mathbb{R}^2$ is the closed unit disk) is defined by

$$\begin{cases} \xi_1 = a_1(\ \ z_1 \sin\theta + z_2 \cos\theta) \\ \xi_2 = a_2(-z_1 \cos\theta + z_2 \sin\theta) \end{cases} \qquad \text{with} \quad \begin{array}{c} -\sqrt{1-z_2^2} \le z_1 \le \sqrt{1-z_2^2}, \\ -1 \le z_2 \le 1 \end{array} \tag{63}$$

which implies

$$\mathrm{d}V(\boldsymbol{\xi}) = a_1 a_2 \, \mathrm{d}z_1 \, \mathrm{d}z_2$$

Now, mappings (62) and (63) are substituted into the integral representation formula (60). Noting that definitions (61), (62) and (63) imply

$$\boldsymbol{\alpha}(\theta)\cdot\boldsymbol{x} = y\cos\theta, \qquad \boldsymbol{\eta}\cdot(\boldsymbol{\xi}-\boldsymbol{x}) = t[z_2 - \boldsymbol{\alpha}(\theta)\cdot\boldsymbol{x}],$$

one first finds, using mapping (63) and the fact that the integrand of the resulting integral over (z_1, z_2) does not depend on z_1, that

$$\int_{\mathcal{B}} e^{\mathrm{i}\boldsymbol{\eta}\cdot(\boldsymbol{\xi}-\boldsymbol{x})} \, \mathrm{d}V(\boldsymbol{\xi}) = a_1 a_2 e^{-\mathrm{i}t\boldsymbol{\alpha}(\theta)\cdot\boldsymbol{x}} \int_{-1}^{1} 2\sqrt{1-z_2^2} \, e^{\mathrm{i}tz_2} \, \mathrm{d}z_2 = a_1 a_2 \frac{2\pi}{t} e^{-\mathrm{i}t\boldsymbol{\alpha}(\theta)\cdot\boldsymbol{x}} J_1(t),$$

where J_1 is the Bessel function of first kind and order 1, the last equality stemming from formula 3.752 of [24] together with the function $z_2 \longmapsto \sqrt{1-z_2^2} \sin k z_2$ being odd. Then,

using the above result into (60) and applying mapping (62), one obtains

$$\begin{aligned}\frac{\mathrm{i}}{(2\pi)^2}\int_{\mathbb{R}^2}\int_{\mathcal{B}}\exp(\mathrm{i}\boldsymbol{\eta}\cdot(\boldsymbol{\xi}-\boldsymbol{x}))\boldsymbol{N}(\boldsymbol{\eta})\otimes\boldsymbol{\eta}\,\mathrm{d}V(\boldsymbol{\xi})\,\mathrm{d}V(\boldsymbol{\eta})\\ =\frac{\mathrm{i}}{2\pi}\int_0^{2\pi}\Big\{\boldsymbol{N}\big(\boldsymbol{\alpha}(\theta)\big)\otimes\boldsymbol{\alpha}(\theta)\int_0^{\infty}e^{-\mathrm{i}t\boldsymbol{\alpha}(\theta)\cdot\boldsymbol{x}}J_1(t)\frac{\mathrm{d}t}{t}\Big\}\,\mathrm{d}\theta\\ =\frac{1}{\pi}\int_{-\pi/2}^{\pi/2}\Big\{\boldsymbol{N}\big(\boldsymbol{\alpha}(\theta)\big)\otimes\boldsymbol{\alpha}(\theta)\int_0^{\infty}\sin\big(t\,\boldsymbol{\alpha}(\theta)\cdot\boldsymbol{x}\big)J_1(t)\frac{\mathrm{d}t}{t}\Big\}\,\mathrm{d}\theta\end{aligned}\tag{64}$$

The last equality above is established by using that (i) $\boldsymbol{\alpha}(\theta)$ is 2π-periodic, (ii) $\boldsymbol{\alpha}(\theta+\pi)=-\boldsymbol{\alpha}(\theta)$ and (iii) $\boldsymbol{N}(-\boldsymbol{\eta})=\boldsymbol{N}(\boldsymbol{\eta})$ ($\boldsymbol{N}$ being homogeneous of degree -2).

The inner integral in (64) in fact admits a known closed-form expression (formula 6.693(1) of [24]), which depends on the value of $\boldsymbol{\alpha}(\theta)\cdot\boldsymbol{x}=y\cos\theta$:

$$\int_0^{\infty}\sin\big(t\,\boldsymbol{\alpha}(\theta)\cdot\boldsymbol{x}\big)J_1(t)\frac{\mathrm{d}t}{t}=\boldsymbol{\alpha}(\theta)\cdot\boldsymbol{x}\qquad 0\le\boldsymbol{\alpha}(\theta)\cdot\boldsymbol{x}\le 1\tag{65a}$$

$$=\boldsymbol{\alpha}(\theta)\cdot\boldsymbol{x}-\sqrt{(\boldsymbol{\alpha}(\theta)\cdot\boldsymbol{x})^2-1}\qquad \boldsymbol{\alpha}(\theta)\cdot\boldsymbol{x}\ge 1\tag{65b}$$

If $\boldsymbol{x}\in\mathcal{B}$, (61) implies that $y\le 1$, and hence that $\boldsymbol{\alpha}(\theta)\cdot\boldsymbol{x}\le 1$ for any θ. From (60), (64) and (65a,b), $\boldsymbol{u}(\boldsymbol{x})$ is then such that

$$\boldsymbol{u}(\boldsymbol{x})=\boldsymbol{x}\boldsymbol{\mathcal{S}}^{\mathrm{int}}:\boldsymbol{E}^{\star},\qquad\boldsymbol{\nabla}\boldsymbol{u}(\boldsymbol{x})=\boldsymbol{\mathcal{S}}^{\mathrm{int}}:\boldsymbol{E}^{\star}$$

where $\boldsymbol{\mathcal{S}}^{\mathrm{int}}$ is the plane-strain interior Eshelby tensor, given by

$$\boldsymbol{\mathcal{S}}^{\mathrm{int}}=\Big\{\frac{1}{\pi}\int_{-\pi/2}^{\pi/2}\boldsymbol{\alpha}(\theta)\otimes\boldsymbol{N}\big(\boldsymbol{\alpha}(\theta)\big)\otimes\boldsymbol{\alpha}(\theta)\,\mathrm{d}\theta\Big\}:\boldsymbol{\mathcal{C}}$$

If $\boldsymbol{x}\in\mathbb{R}^2\setminus\bar{\mathcal{B}}$, (61) implies that $y>1$. Let $\bar\theta=\arccos(1/y)$, so that the subset of $\theta\in[-\pi/2,\pi/2]$ where $\boldsymbol{\alpha}(\theta)\cdot\boldsymbol{x}\ge 1$ is $\theta\in[-\bar\theta,\bar\theta]$. In that case, using (60), (64) and (65a,b) and differentiating the resulting expression of $\boldsymbol{u}(\boldsymbol{x})$ with respect to $\boldsymbol{x}$, one finds

$$\boldsymbol{\nabla}\boldsymbol{u}(\boldsymbol{x})=\boldsymbol{\mathcal{S}}^{\mathrm{ext}}(\boldsymbol{x}):\boldsymbol{E}^{\star}$$

with the plane-strain exterior Eshelby tensor $\boldsymbol{\mathcal{S}}^{\mathrm{ext}}(\boldsymbol{x})$ given by

$$\boldsymbol{\mathcal{S}}^{\mathrm{ext}}(\boldsymbol{x})=\boldsymbol{\mathcal{S}}^{\mathrm{int}}-\frac{2}{\pi}\Big\{\int_{-\bar\theta}^{\bar\theta}\Big[\frac{(\boldsymbol{\alpha}(\theta)\cdot\boldsymbol{x})}{\sqrt{(\boldsymbol{\alpha}(\theta)\cdot\boldsymbol{x})^2-1}}\boldsymbol{\alpha}(\theta)\otimes\boldsymbol{N}\big(\boldsymbol{\alpha}(\theta)\big)\otimes\boldsymbol{\alpha}(\theta)\Big]\,\mathrm{d}\theta\Big\}:\boldsymbol{\mathcal{C}}$$

Even though this representation of the 2D general Eshelby tensor is valid, is not suited for numerical evaluation due to the term $1/\sqrt{(\boldsymbol{\alpha}\cdot\boldsymbol{x})^2-1}$, which is (weakly) singular at the endpoints $\theta=\pm\bar\theta$. We recast it into a form suitable for numerical quadrature by setting

$$\sin\theta=\sqrt{1-y^{-2}}\sin w,\qquad\theta\in[-\bar\theta,\bar\theta],\ w\in[-1,1]$$

Then, since $\boldsymbol{\alpha}(\theta)\cdot\boldsymbol{x}=y\cos\theta$, one easily finds that

$$(\boldsymbol{\alpha}(\theta)\cdot\boldsymbol{x})\,\mathrm{d}\theta=\sqrt{y^2-1}\cos w\,\mathrm{d}w,\quad\sqrt{(\boldsymbol{\alpha}(\theta)\cdot\boldsymbol{x})^2-1}=\sqrt{y^2-1}\cos w$$

Consequently, $\boldsymbol{\mathcal{S}}^{\mathrm{ext}}(\boldsymbol{x})$ is now expressed as

$$\boldsymbol{\mathcal{S}}^{\mathrm{ext}}(\boldsymbol{x})=\boldsymbol{\mathcal{S}}^{\mathrm{int}}-\frac{2}{\pi}\Big\{\int_{-\pi/2}^{\pi/2}\Big[\boldsymbol{\alpha}(\theta(w))\otimes\boldsymbol{N}\big(\boldsymbol{\alpha}(\theta(w))\big)\otimes\boldsymbol{\alpha}(\theta(w))\Big]\,\mathrm{d}w\Big\}:\boldsymbol{\mathcal{C}}$$

where the integral can now be evaluated by usual quadrature rules.